TECHNISCHE UNIVERSITÄT WIEN
Vienna University of Technology

MASTER THESIS

Intracellular Bioorthogonal Chemistry

conducted at the

Institute of Applied Synthetic Chemistry

Vienna University of Technology

under the supervision of

Univ.Prof. Dipl.-Ing. Dr.techn. Johannes Fröhlich

Projektass. Dipl.-Ing. Dr.techn. Hannes Mikula

by

Emanuel Sporer, BSc.

„Damit das Mögliche entsteht,
muss immer wieder das Unmögliche versucht werden“

Hermann hesse

Abstract

Bioorthogonal reactions can be pivotal in medicinal therapeutics and diagnostics. In essence, extracellularly binding substances like antibodies and peptides, which are often used as targeting agents, are coupled with a bioorthogonal reaction agent. The most popular combination nowadays is the inverse electron demand Diels-Alder reaction between a *trans*-cyclooctene and a tetrazine.

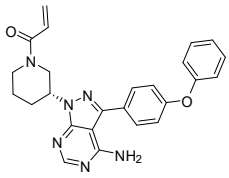

The motivation behind this thesis is to establish that this kind of reaction is not only able to be used for *in vitro* reactions but as well for intracellular reactions. Therefore, an intracellular targeting agent, ibrutinib, was synthesized. It binds covalently to Bruton tyrosine kinase (BTK), which is expressed by chronic lymphocytic leukemia (CLL) and other leukemia diseases. Through the introduction of an amine-group, this targeting agent can be modified without inhibiting its ability to covalently bind to BTK. Besides this classic click reaction, bioorthogonal bond cleavage reactions have recently been discovered, e.g. click-to-release chemistry, which was used in combination with the ibrutinib model to develop a tool to study intracellular bioorthogonal elimination. To enable release upon tetrazine ligation, a leaving group was introduced at the allylic position of TCO. This reaction can be employed to achieve intracellular release of a variety of compounds (e.g. drugs), which is thus of increasing interest. As a proof-of-concept, within this thesis three different ibrutinib derivates were prepared in multistep synthetic sequences and evaluated. We were able to show that bioorthogonally modified ibrutinib still specifically binds to BTK. Intracellular reactions were confirmed by cell uptake measurements using radiolabeled tetrazines. The click-to-release reaction was studied and confirmed in vitro applying a drug-TCO-dye conjugate.

Consequently, the ibrutinib model was shown to be a valuable tool to study intracellular bioorthogonal reactions. This will not only enable the development of imaging techniques that can be used for diagnostics and to attain a better understanding of biosystems, but moreover allow us to investigate intracellular bioorthogonal elimination reactions towards theranostic applications.

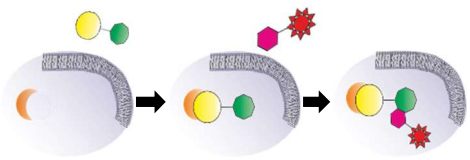

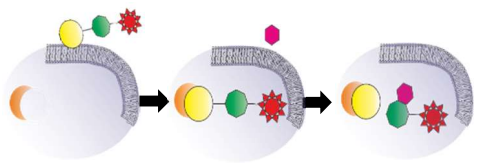

Kurzfassung

Bioorthogonale Reaktionen spielen in der Medizin sowohl in der Diagnostik wie auch in der Therapie schon heute eine zentrale Rolle. Dabei wird meist auf extrazellulär bindende Substanzen (z.B. Antikörper) zurückgegriffen, welche mit einer zur bioorthogonalen Reaktion fähigen Funktionalität modifiziert werden. Dabei nimmt die Diels-Alder Reaktion zwischen einem *trans*-Cycloocten und dem Tetrazin aufgrund der sehr hohen Reaktions-geschwindigkeit und der Biokompatiblität der einzelnen Substanzen eine besonders hoffnungstragende Rolle ein.

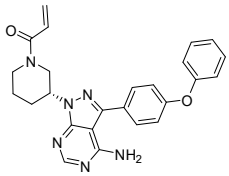

Das Ziel dieser Arbeit ist die Entwicklung eines Modelsystems, das die Untersuchung von intrazellulären bioorthogonalen Reaktionen ermöglicht. Als Zielreagens wurde der zugelassene Wirkstoff Ibrutinib verwendet. Dieser Inhibitor bindet kovalent an Bruton Tyrosin Kinase (BTK) als intrazelluläres Target. BTK wird bei chronischer lymphatischer Leukämie und anderen leukämischen Erkrankungen exprimiert.

Durch die Einführung einer Aminogruppe an einer nicht für die selektive Bindung verantwortlichen Stelle, sollte Ibrutinib mit bioorthogonalen Gruppen modifiziert werden, ohne eine kovalente und selektive Bindung an BTK zu verhindern. Neben der klassischen Click-Reaktion sollten auch bioorthogonale Eliminationsreaktionen, wie z.B. die sogenannte „click-to-release“-Reaktion mithilfe des Ibrutinib-Modells untersucht werden. Dazu wird in allylischer Position eine Abgangsgruppe in das TCO eingeführt, welches bei der folgenden Reaktion mit einem Tetrazin abgespaltet wird. Somit kann dieses Model auch dazu dienen, Wirkstoffe direkt in der Zelle frei zu setzen.

Im Rahmen dieser Arbeit wurden drei verschiedene Ibrutinib-Konjugate in mehrstufigen Sequenzen synthetisiert und anschließend evaluiert. Dabei konnte gezeigt werden, dass trotz der Modifikation eine hohe Selektivität für eine kovalente Bindung an BTK erreicht wird. Intrazelluläre bioorthogonale Ligation wurde mithilfe von radioaktiv markierten Tetrazinen nachgewiesen. Zudem wurde ein Ibrutinib-TCO-Fluorophor Konjugat entwickelt, welches zur Untersuchung intrazellulärer Eliminationsreaktionen angewendet werden kann.

Das entwickelte Modell ermöglicht daher zukünftige Entwicklungen sowie Untersuchungen im Bereich der Diagnostik (z.B. medizinische Bildgebung), als auch neuartige Strategien für die selektive Freisetzung von Wirkstoffen (therapeutische Anwendungen).

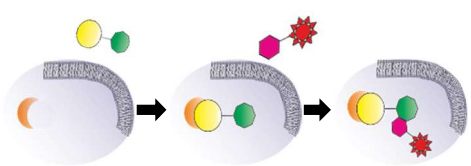

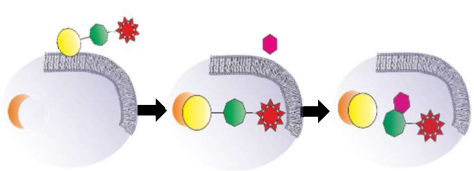

Acknowledgement

First of all, I would like to thank *Univ. Prof. Dipl.-Ing. Dr. Johannes Fröhlich* for giving me the opportunity to accomplish this master thesis within his research group.

My sincerest appreciation also goes to *Ass. Prof. Dipl.-Ing. Dr. Christian Hametner* for the conduction of numerous NMR experiments and his readily given support concerning this technology.

Furthermore, I want to express my gratitude to my supervisor *Hannes Mikula* who always has a sympathetic ear for my chemical problems but as well for any organizational difficulties.

Special thanks to *Stefan Kronister* for his help and advice in LC-MS measurements, Grace purifications, for being a great bench neighbor, and for his overall helpfulness in all respects.

I am grateful to *Max Haider* for all his amazing help in synthetic questions and for his relaxing nature.

I would also like to thank *Christoph Denk* for his help with cell-culture and radiolabeling but as well for the very nice and often productive talks with him.

Markus Schwarz is another person to whom I am very grateful, because he is the one who introduced me into this amazing research group.

Thanks to all further members of the FGHF! You create the working atmosphere that allows new ideas to come to mind and the constructive climate of discussion that is essential in order to take a step forward. Namely: *Babara Sohr, Stefan Lexmüller*, *Paul Kautny, Florian Glöcklhofer, Dennis Svatunek, Brigitte Holzer, Thomas Kader, Dorian Bader, Martin Wilkovitsch, Walter Kuba, Julia Weber, Philip Skrinjar*

Of course, I want to thank my partner Christina for being there for me in chemical, personal, and all other questions.

Last but not least, special gratitude goes to my brothers Matthias and Florian and to my parents Eduard and Anita for their incredible support throughout my studies in hard and easy times and for being the source of who I am.

Abbreviations

PEG	Polyethylenglykol
BTK	Bruton´s Tyrosin Kinase
Brine	saturated aqueous NaCl solution
CC	column chromatography
CFC	copper-free click chemistry
DCM	dichlormethane
DIPEA	diisopropylethylamine
DMF	N,N-dimethylformamide
EA	ethyl acetate
ESI	electrospray ionization
HBTU	N,N,N′,N′-tetramethyl-O-(1H-benzotriazol-1-yl)uronium hexafluorophosphate
LC-MS	liquid chromatography – mass spectrometry
FBS	fetal bovium serum
MeOH	methanol
MS	mass spectrometry
MTBE	methyl-tert-butylether
NMR	nuclear magnetic resonance
PE	petroleum ether (hexanes)
r.t.	room temperature
TCO	*trans*-cyclooctene
THF	tetrahydrofurane
ACN	acetonitrile

General explanatory notes

Literature References

Literature references are distinguished as superscript Arabic numerals in square brackets.

Nomenclature

Names of compounds that are not described in the chemical literature were created according to the nomenclature rules of Chemical Abstracts. Therefrom excluded or unknown compounds in the literature as well as reagents and solvents, respectively are partially described with simplified, trivial or trading names.

Table of Contents

I. General Schemes

I.1. Ibrutinib-Derivates

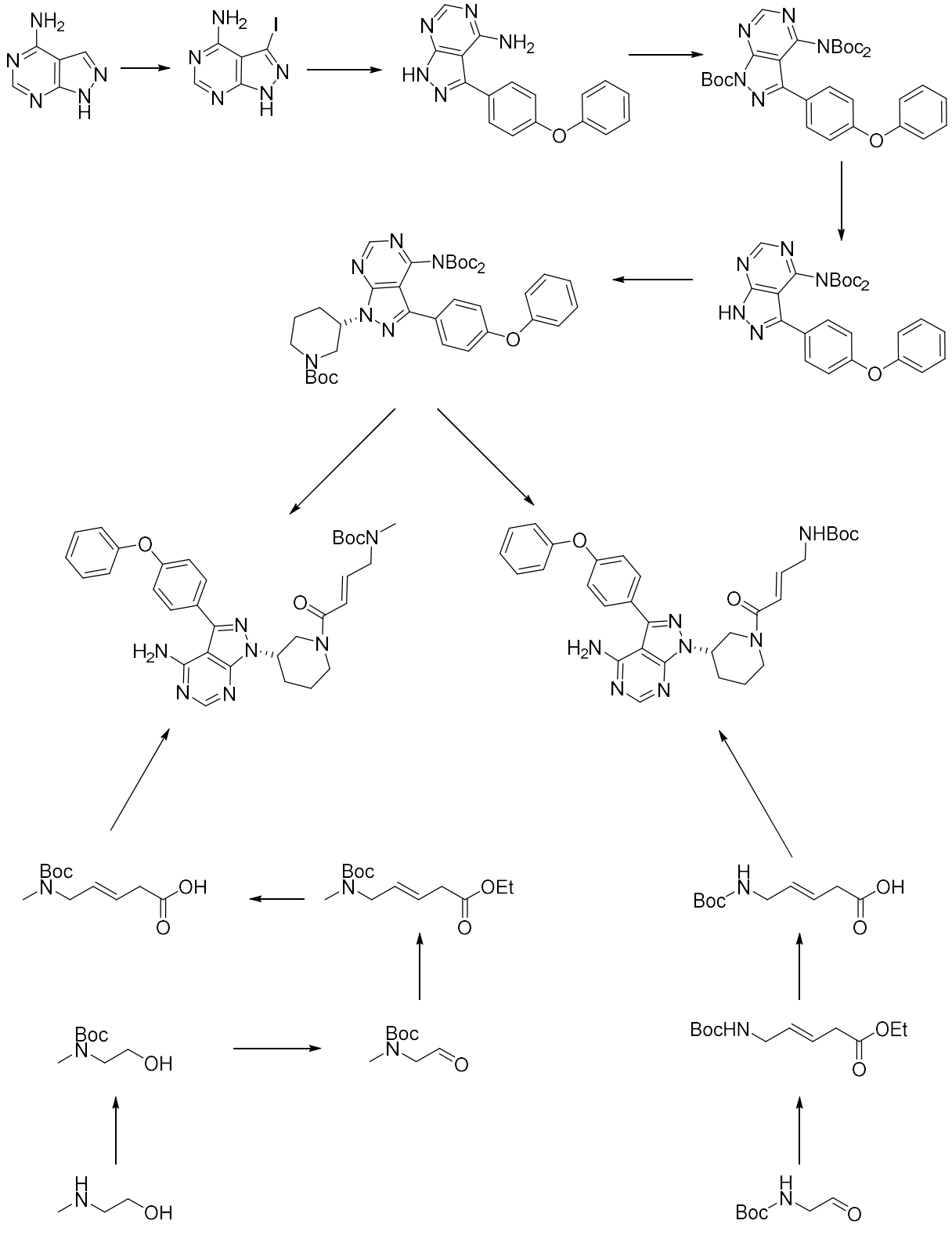

I.2. Multifunctional Release TCO (m-TCO)

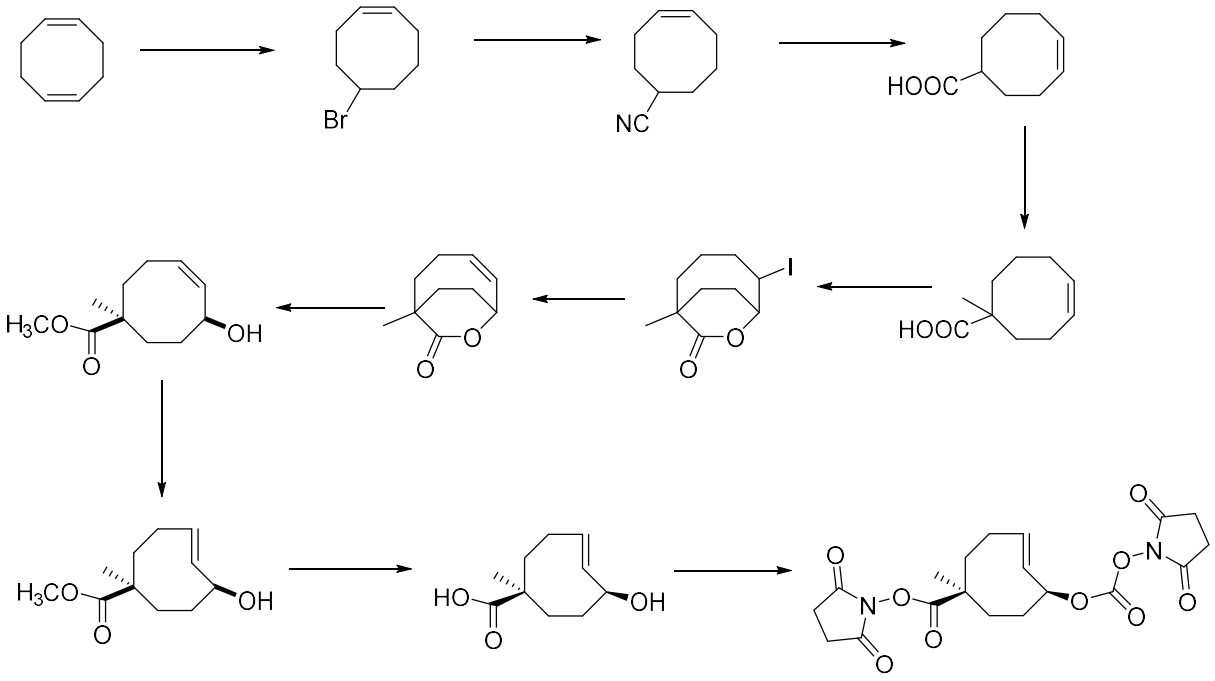

I.3. d-TCO combined with Ibrutinib-Derivate

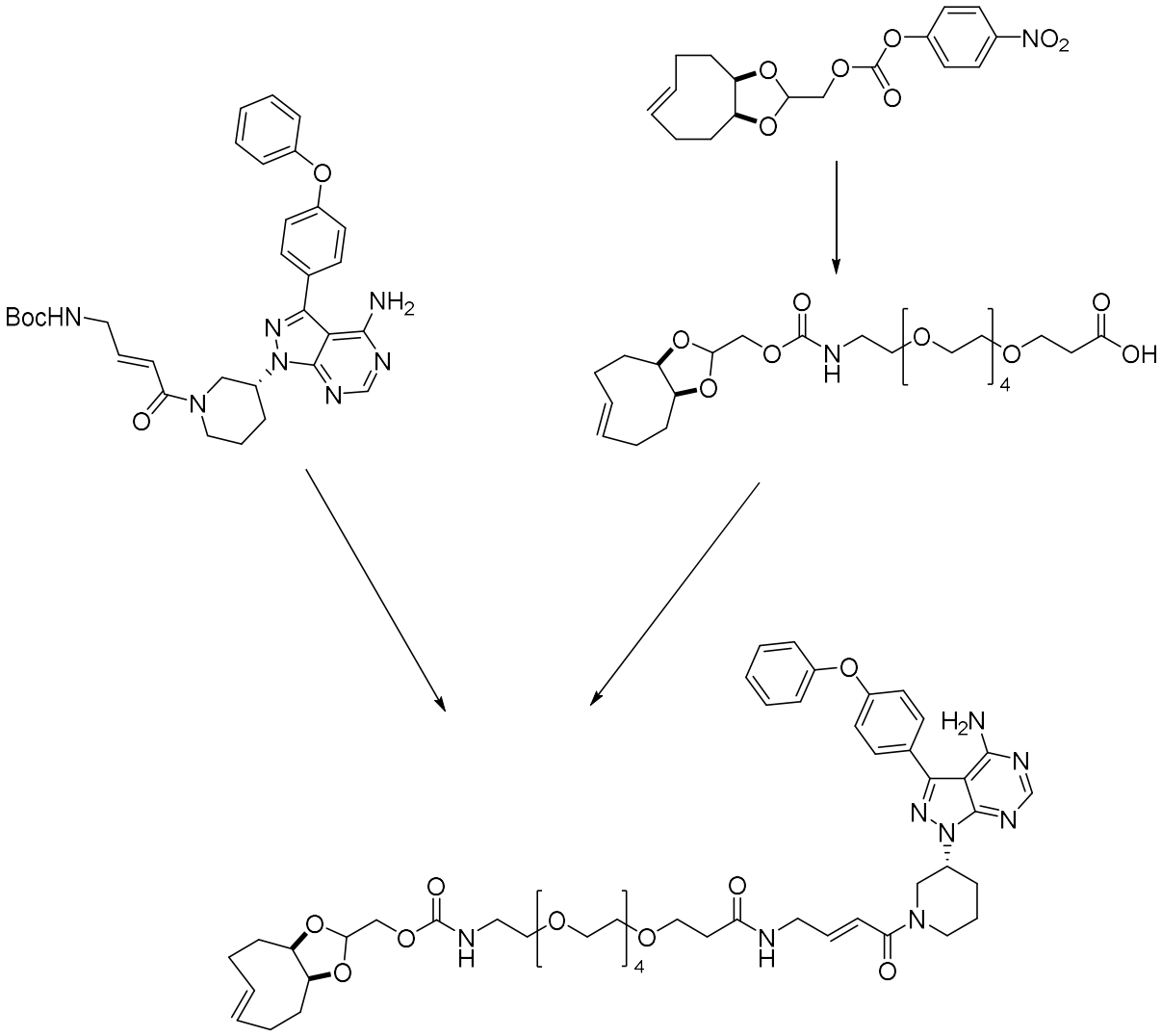

I.4. Standard-TCO combined with Ibrutinib-derivate

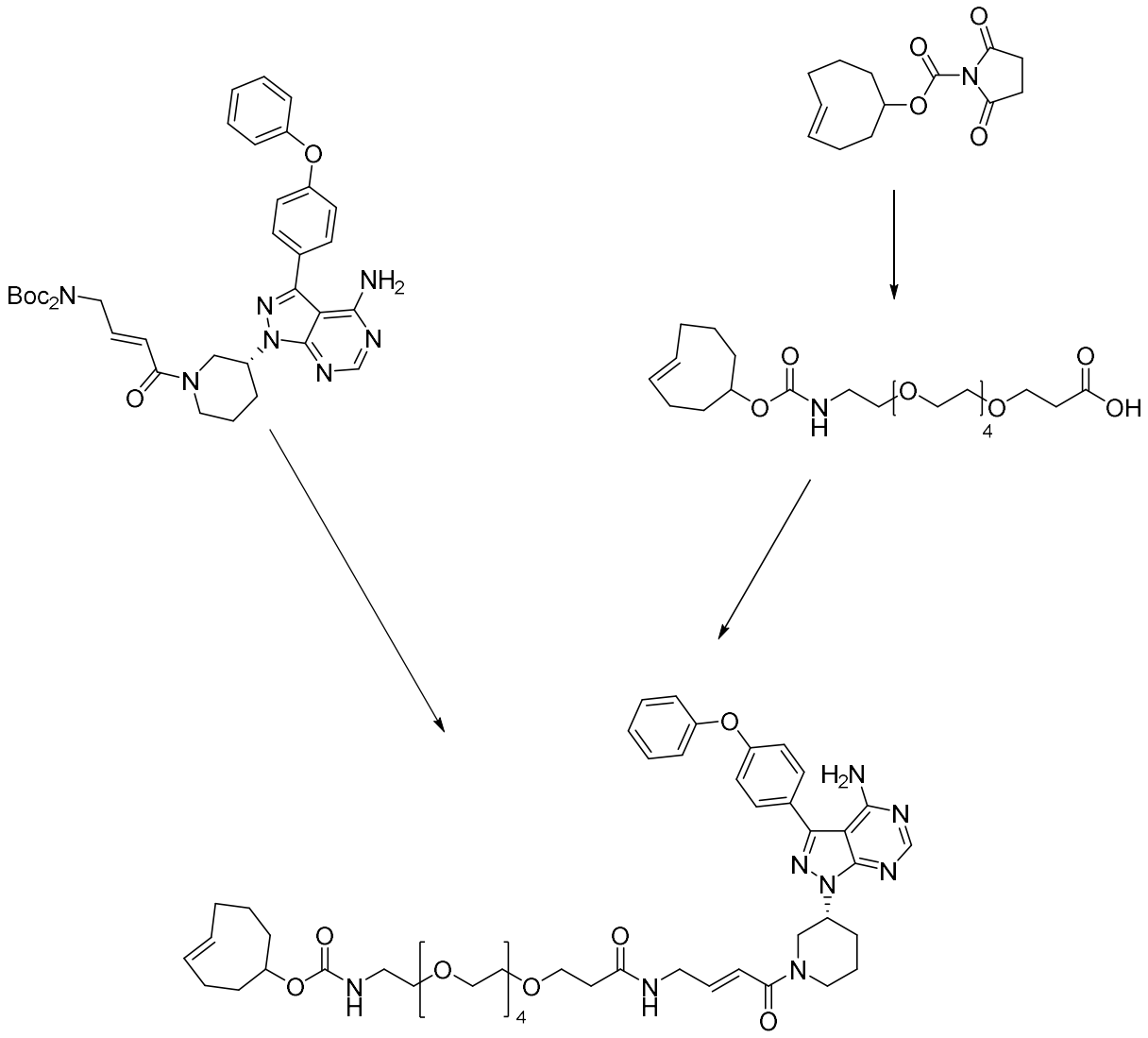

I.5. m-TCO combined with Ibrutinib-derivate and SIR-dye

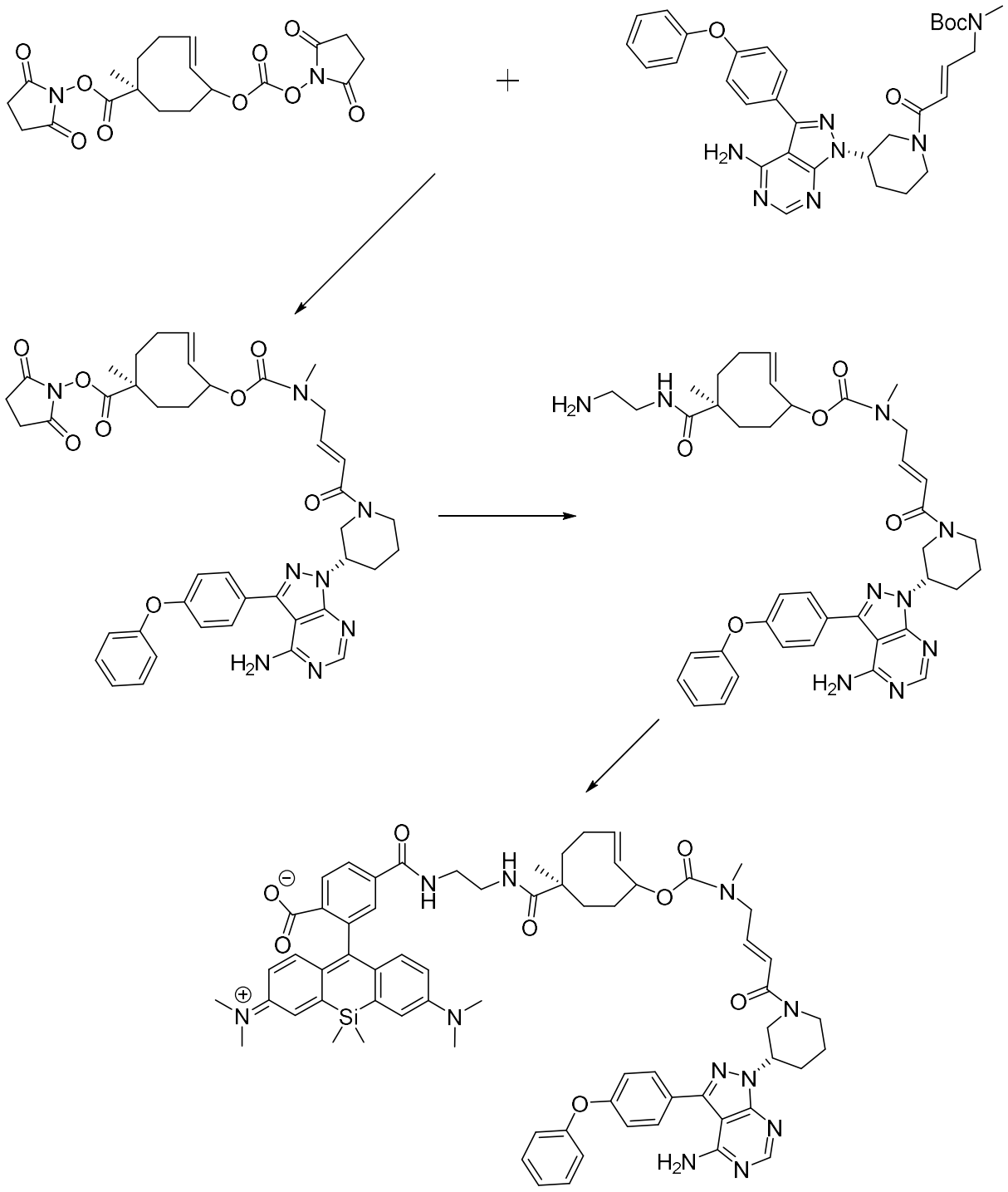

II. Introduction

II.1. Bioconjugation

There are various methods in organic synthesis to design bioconjugates, covalently as well as non-covalently, which leads to a tremendous amount of applications like the discovery of new biomolecules, the elucidation of complex biological processes, medical diagnostics and therapy (*e.g*. bioconjugates with isotope labels, fluorescent dyes, affinity tags, biotin, Elisa), life sciences, microelectronics, and material science fields. [1][2][3]

II.1.1 Definition of Bioconjugation

Bioconjugation is fundamentally the binding between two molecules, where in most cases at least one of them is a fragment or a derivate of a biomolecule. Nevertheless, it is possible for the complete bioconjugate to be formed synthetically, if it has applications in a biological system. Modification of a biological moiety with a synthetic group is a further possible method to form a bioconjugate. All these techniques are important to understand the role of molecules in biological systems[1][2].

II.1.2 Design Strategy of Bioconjugates

There are many different methods to design bioconjugates, as a large variety of reactions are available. Nevertheless, every part of the molecule has an essential role to perform in the biosystem and thus it is very important to adjust them to their final applications. For example, if the bioconjugate is needed for an assay, a binding mechanism (e.g. antibody) and a possibility to visualize (e.g. fluorescent dye) the structure is necessary. Therefore, it is very helpful to use parts which are already explored in similar applications. For *in vivo* imaging applications for instance, the fluorescent dye should have spectral properties in the far red to near infrared. For cell applications, however, the emission properties from the dye should be somewhere between near infrared to the UV region.[1]

II.1.2.1 Role of Fluorescent Dye in bioconjugates

The hydrophobicity and hydrophilicity of the components plays an important role. Thus, sometimes it is recommended to use a hydrophilic dye to prevent the molecule from non-specific binding or from aggregation with an antibody. On the other hand, this hydrophobic non-specific binding is desired when considering interactions with biomolecules or with the surface in assays. Another big advantage of less charged dyes is that they preferably penetrate membrane structures to reach a desired target. Nevertheless, it is very difficult to find the right balance between hydrophobicity and hydrophilicity. Therefore, testing of several different dyes is frequently the best way to find the optimum.[1]

II.1.2.2 PEGylation

Another adequate tool to design the properties of bioconjugates are the linker arms. For example, some linkers contain hydrophobic parts like aliphatic or aromatic moieties, which leads to a more hydrophobic molecule. On the other hand, you can use this tool to get a more hydrophilic bioconjugate as well. One well-established technique is PEGylation.[1][3]

PEGylation means the introduction of one or more short, discrete polyethylenglycole (PEG)-chains onto the biomolecule. This kind of modification has an immense impact on the characteristics of the bioconjugate like increasing water-solubility. Reduced immunogenicity due to the length of the PEG-group and the resulting shielding property as well as increased hydrodynamic volume and reduced excretion of the drug through the kidney are additional effects. These points are the reason for a higher serum half-life of the bioconjugates *in vivo*. Consequentially, lower toxicity and a higher thermal and mechanical stability are achieved[1][3]. It is noteworthy that this PEG-chain augments passive targeting towards solid tumors through the enhanced permeability and retention effect[4].

II.2. Bioorthogonal Ligation

In recent years, more and more methods to make covalent bindings between markers and biopolymers have been developed[5]. The first reaction of this kind, called bioorthogonal ligation, was discovered by Bertozzi[6]. It is a reaction which does not interfere with biological systems and has no side effects on the cellular mechanism[7]. Reactions which are designed to take place in living systems require a lot of parameters to be constant (pH, temperature, solvent etc.) in comparison to a conventional chemical reaction. Therefore, only the structure of the reaction components influences its properties such as speed and selectivity. Thus, some prerequisites for bioorthogonal reactions have been named[7]:

1. All components of the reaction like reagents and product, have to be metabolically stable, non-toxic, and should not interact with any component of the biosystem.
2. The reaction should be highly specific with fast kinetics at low concentrations.

It is remarkable that only a small number of reactions in the wide field of organic chemistry show characteristics of a bioorthogonal reaction, but none fulfills all the requirements.

II.2.1. Historical Development

The first invention in the direction of bioorthogonal reactions was made by Staudinger *et al*. in the year 1919 with the reaction between an azide and triaryl phosphane to form iminophosphoranes[8]. The next step was the modification of the Staudinger reaction to the tracerless Staudinger-ligation developed in 2000 by Bertozzi *et al.* (Figure 1)[9].

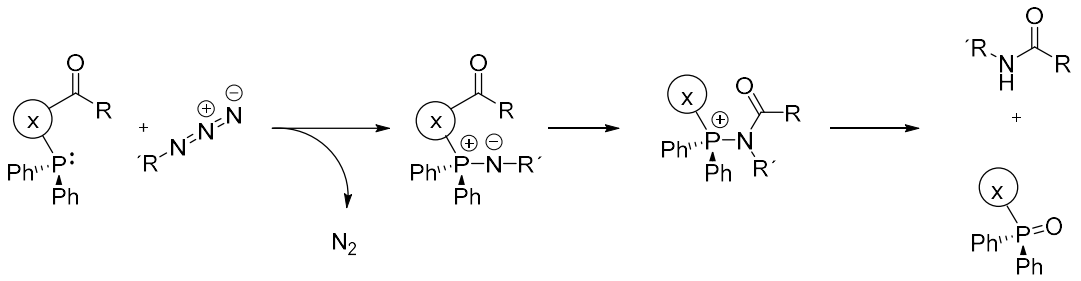

Figure 1: Tracerless Staudinger-ligation

The next noteworthy development was the design of the first click reaction in 2002 by Sharpless *et al.*, based on the Huisgen 1,3-dipolar cycloaddition between an azide and an alkyne[10]. In its classical form, the reaction has limited applications in biosystems due to the high temperatures and the low reaction rates[11]. Therefore, Sharpless modified the reaction by adding Cu(I) as a catalyst (Figure 2). This introduced regiospecificity to yield 1,4-disubstituted 1,2,3-triazole and the reaction rate increased as well[10]. On the other hand, due to the definition of bioorthogonal reactions by Bertozzi *et al.*, this reaction is not a bioorthotogonal ligation because of the toxicity of copper to bacterial and mammalian cells[11].

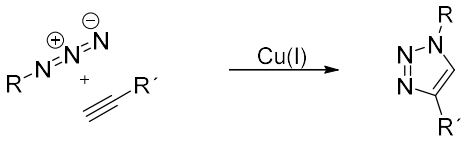

Figure 2: Click reaction between azide and alkyne

To solve this problem, Bertozzi *et al.* finally found a copper free click reaction. This reaction is again between an azide and alkyne but in contrast to the reaction from Figure 2, the following bioorthotogonal ligation has a ring-strained alkyne which one can see in Figure 3.

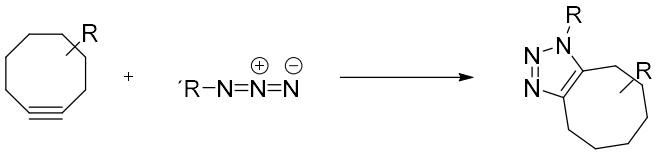

Figure 3: First bioorthogonal click reaction

Due to the ring strain of the alkyne [12] and the resulting acceleration of this Huisgen reaction, the copper catalyst is not needed anymore to get a regiospecific product. This reaction can occur without copper catalysis and therefore no component of the reaction is toxic. The reaction rate, however, cannot compete with the Cu(I) catalyzed reaction.

To prevent aforementioned problems, Weissleder *et al.* and Fox *et al.* independently describe a new kind of ring-strained cycloaddition (Figure 4)[13][14]. This reaction is an inverse electron demand Diels-Alder (IEDDA) reaction between a ring-strained Cyclooctene, the most reactive alkene[15], and a 1,2,4,5 tetrazine. An intermediate is formed which rearranges by release of the byproduct N_2 to a 4,5-dihydropyridazinee. Finally, this product can tautomerize in protic solvent to the final product[14].

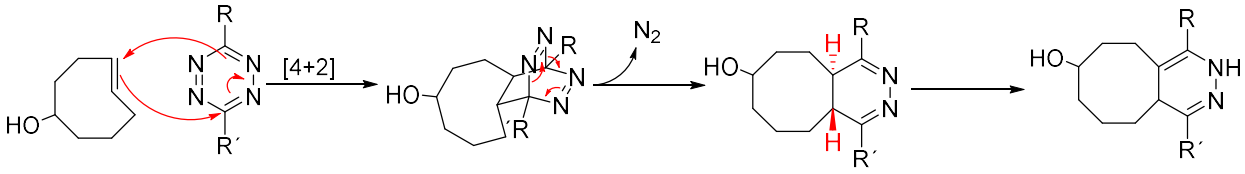

Figure 4: Tetrazine ligation

The main advantages are the high reaction rate between the tetrazine and the ring-strained alkene[15] and the compatibility of the Diels-Alder reaction with aqueous conditions[16]. To get a better overview of the described reaction, the next chapter explains the principle of tetrazine ligation in more detail.

II.3. Tetrazine Ligation

As already recognized, a bioorthogonal reaction should be able to take place in biosystems. Therefore, good *in vivo* stability is necessary. But on the other hand, a high reaction rate is indispensable as well.

The major advantage of using a Diels-alder-reaction is its acceleration under aqueous conditions[17]. Nonetheless, not every component (for example several tetrazines) can be applied to bioconjugation because they are not stable in water or react with it[15]. Thus, it is necessary to find a good balance between high reaction rate and good *in vivo* stability in order to attain an applicable bioorthotogonal reaction. Modification of these properties is possible by tuning of diene and dienophile

II.3.1. Impact of the Reaction Components

A classic Diels-Alder reaction that is very fast and takes place under mild conditions was discovered in 1928[18]. To attain a higher efficiency of this reaction, an electron rich diene and an electron-poor dienophile is desirable. The reason for the acceleration of this reaction can be attributed to the energy level of the diene's highest occupied molecular orbital (HOMO) and the dienophile's lowest unoccupied molecular orbital (LUMO)[19]. In contrast, in 1949 the IEDDA was described by Bachmann and Deno[20] and introduced the reaction between an electron rich diene and an electron-poor dienophile.

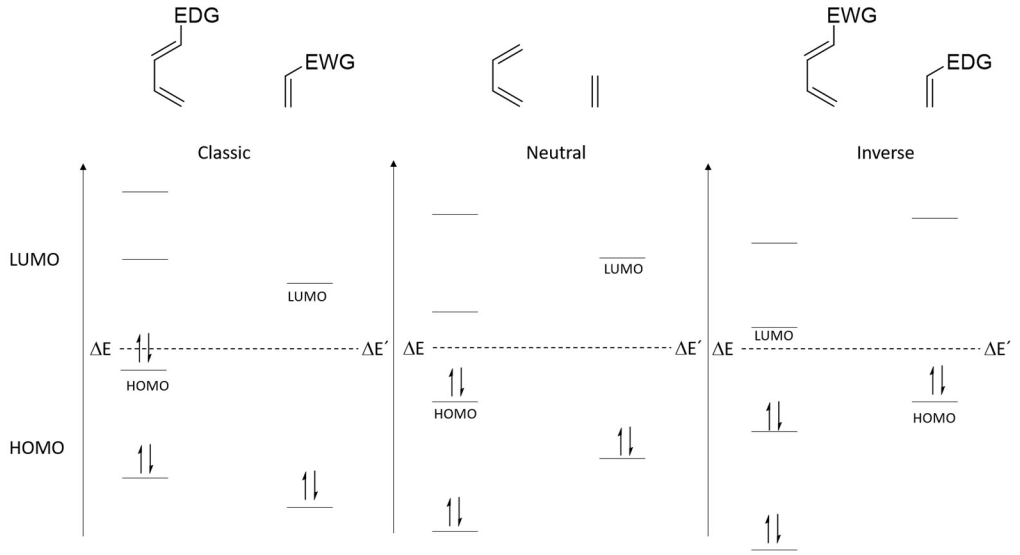

Figure 5: Schematic energy diagram to illustrate the electron effects of the LUMO and HOMO

As one can see in Figure 5, the IEDDA is controlled by the interaction between the HOMO of the dienophile and the LUMO of the diene[21].

In this special case of the tetrazine ligation, the heteroatom in the tetrazine lowers the energy of the LUMO due to the electronegativity of nitrogen. Electron donating groups accordingly raise the energy of the dienophil's HOMO. Therefore, the gap between the two decreases, the orbitals can overlap better, and the reaction rate is elevated.

II.3.1.1 Diene

As mentioned previously, the components of a bioorthogonal reaction have to fulfill different prerequisites like high reaction kinetics, good water solubility, and stability.

As predicted, tetrazines with electron withdrawing groups on position 3 and 6 show faster kinetics when compared to tetrazines which have electron donating groups. However, these effects are not the only ones which influence the reaction-rate of the diene. The tetrazine with hydrogen on position 3 and 6 is much faster than expected. This indicates that steric hindrance significantly contributes to the reaction rate[22].

The next necessary characteristic is conceivable as well. Less polar groups like 3,6 diaryl tetrazines have shown lower water-solubility than the dienes which are substituted with methyl or hydrogen[22].

But on the other hand, excessive use of electron withdrawing moieties is counterproductive. The problem is the loss of stability, which makes them unsuitable for reactions[22]. To summarize, it is vital to find a suitable modification for each specific application and to utilize an appropriate compromise between electron withdrawing and donating functionality.

II.3.1.2 Dienophile

The second important part of the tetrazine ligation is the TCO, which acts as the dienophile in the IEDDA-reaction. Accordingly, the TCO is the second crucial part in finding a well-fitted bioorthogonal reaction.

So far, a lot of different publications have already discussed faster reaction kinetics due to the TCO. One possibility to modify the reactivity of the dieonphile is to raise the HOMO and minimize the gap between the $HOMO_{dienophile}$ and the $LUMO_{diene}$. Briefly, olefinic dienophiles have much higher reaction rates in comparison to acetylenic dienophiles due to the electron withdrawing effect of triple bonds[23].

The second important approach to modifying reaction kinetics is the ring strain. Sauer *et al.* described the reaction between tetrazines and different alkenes and find the following results: higher ring strain corresponds to higher reaction rate (cyclopropane > cyclobutene > cyclopentane > cycloheptane > Cyclooctene > cyclohexene)[24]. Furthermore, there is a tremendous difference between *cis*-Cyclooctenes and TCOs. The latter are even faster than cyclopropanes[24].

With the aim of discovering an even faster bioorthogonal reaction, Fox and coworkers studied different conformations of the TCO. The standard and lowest energetic conformation of TCOs is the crown conformation, which is visualized in Figure 6. Consequently, a TCO which is forced into a half-chair conformation trough a *cis*-propylene was pursued. This half chair conformation has a 5.9 kcal\mol higher energy[25] making it the fastest TCO to date.

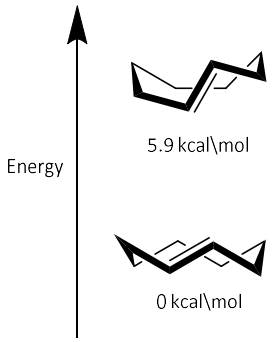

Figure 6: Schematic energy diagram of crown and half-chair conformation

This so called s-TCO has one big disadvantage in the use for a bioorthogonal reaction: it is not water-soluble. Therefore, again Fox *et al.* presented a new TCO (d-TCO) 6 years later. This one has a half-chair conformation as well, provoked trough a *cis*-dioxolan[26], which one can see in Figure 7.

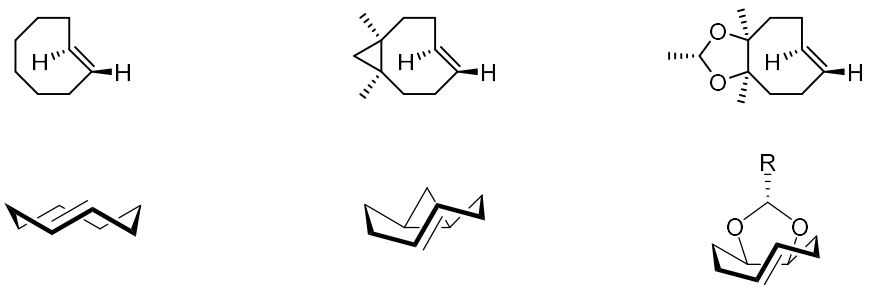

Figure 7: different TCOs (from left to right: standard-TCO, s-TCO, d-TCO) and their conformations

With the introduction of this moiety, they achieved, besides the half chair conformation, a better water solubility due to the two oxygen atoms in the functionality as well as a higher stability[26].

To summarize, a very fast, highly water soluble and stable TCO was developed, which fits very well for different applications for *in vivo* use.

II.3.2 Modification of the Tetrazine Ligation

As mentioned in the previous chapter, the described reaction is an addition reaction between a tetrazine and a TCO. However, in chemistry six different main tools to synthesize exist[27] (substitutions, additions, eliminations, rearrangements, oxidations and reductions, and their combinations). Next to the addition reaction, the substitution- reaction has rapidly emerged in the last years (Figure 8).

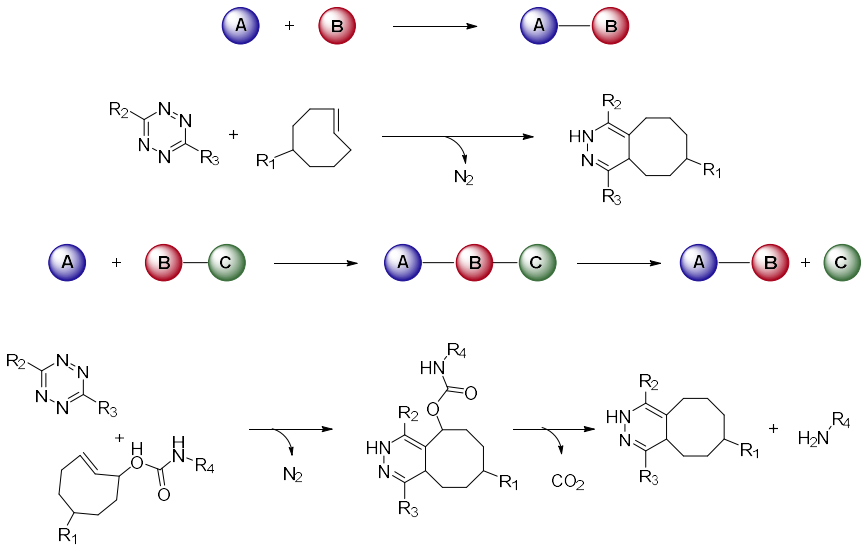

Figure 8: Mechanism of the addition (click) reaction and the substitution (click-to-release) reaction

In order to achieve a well-functioning reaction, Robillard and co-workers focused on the fastest already know bioorthogonal click reaction (an IEDDA-reaction), the tetrazine ligation. To design an elimination- substitution reaction, they added a carbamate leaving in allylic position on the TCO[28]. This type of reaction already has some applications such as antibody drug conjugation release[29]. The following chapter focuses on this reaction and gives some information in detail.

II.3.2.1 Click-to-release

This reaction has the same first two steps as described for the click-reaction. The first step being the addition of the tetrazine to the TCO to attain the 4,5-dihydropyrazine, which tautomerizes to the 1,4-dihydropyrazin[14] predominately under aqueous conditions[30]. This is the starting point for the release reaction. However, specific properties are required to enable the click-to-release reaction. It makes sense that a group with the ability to release is needed. Therefore, we introduce a leaving group to the TCO (Figure 9).

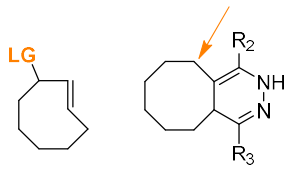

Figure 9: Requirements for the click-to-release reaction

This moiety, a carbamate or carbamothioate group[31], has to be in allylic position. After the click reaction takes place, the further steps are as follows. The 1,4-dihyropyrazine can undergo hydroxylation, which provokes a release of the CO_2 group and results in releasing a NH_2 substituted leaving group. The latter rearranges to the favored aromatic pyridazine to get the final product which is pictured in Figure 10.

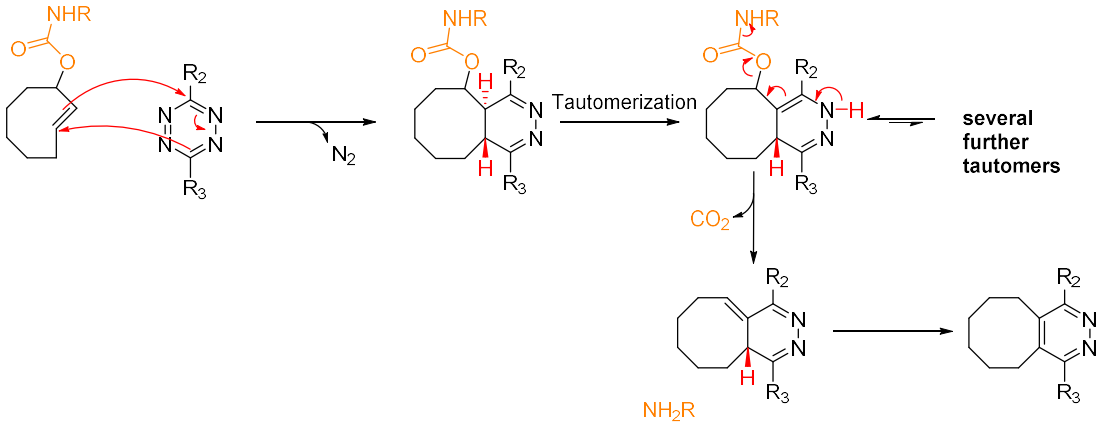

Figure 10: Mechanism of the click-to-release reaction

To attain information about the reaction rate of this click-to-release reaction, Chen *et al.* have published results with different tetrazines. In accordance to expectation, the standard click reaction is accelerated with electron withdrawing groups on the tetrazine due to the lower LUMO of the diene. However, it is noteworthy that an electron withdrawing group reduces the reaction rate of the elimination step[32] (Figure 11)

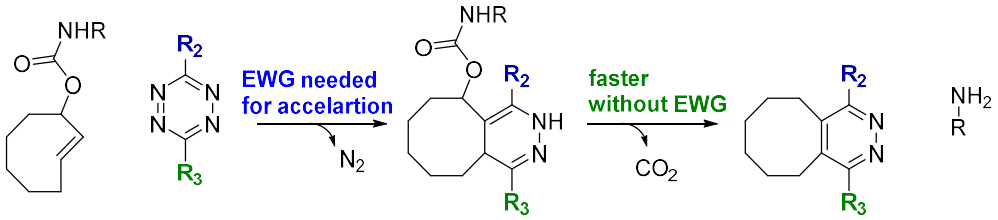

Figure 11: Influence of the diene on the click-to-release reaction

Consequently, the most promising tetrazines are unsymmetrical ones. However, the addition is not stereospecific, which results in different reaction rates of the elimination step. One further effect, which influences the yield and reaction rate of the substitution reaction is an intramolecular attack. This intramolecular nucleophilic attack, which is illustrated in Figure 12, is followed by a dead end. As a result, no release reaction can take place and the yield is negatively affected. To prevent this problem, a methyl-group has to be introduced into the release functionality to transform the secondary amine into a tertiary amine. Thus, the intracellular nucleophilic attack cannot take place anymore[33].

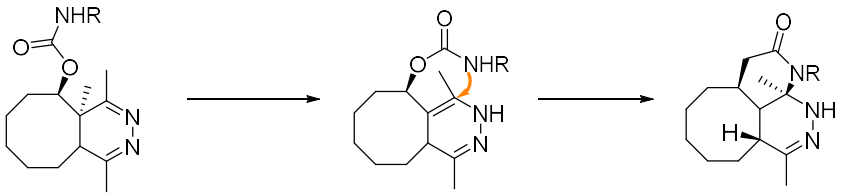

Figure 12: Intramolecular side-reaction of the click-to-release reaction which leads to a dead-end

The next chapter will provide insight into the procedure for transforming a *cis*-cyclooctene into a TCO.

II.4. Isomerization

The formation of TCO from *cis*-Cyclooctene is a vital step towards the components for the tetrazine ligation. A lot of different reactions are already known in literature; for example multistep synthesis over an epoxide and a following elimination[34].

In contrast to these reactions, the photoisomerization of *cis*-cyclooctene is a method to synthesize TCOs directly in one step[35]. *Cis*-cyclooctene can be irradiated with UV-C at 254 nm, which results in an equilibrium between the *cis*-Cyclooctene and the TCO if a singlet sensitizer (*e.g.* methylbenzoate) is present[36][37]. To acquire a pure product, one of the products has to be removed from the equilibrium. One possible method is utilizing silver, as the TCO can form stable complexes with Ag^+ contrary to the *cis*-cyclooctene as shown in Figure 13.

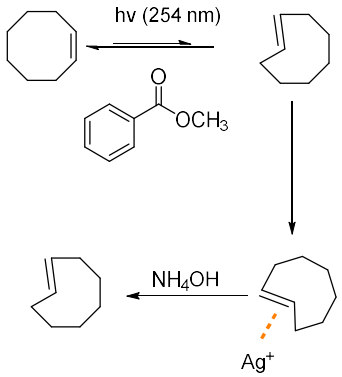

Figure 13: Equilibrium between cis-Cyclooctene and TCO

To take advantage of this, the reaction mixture flows through a cartridge filled with modified silica ($AgNO_3/SiO_2$) to trap the TCO in the cartridge and shift the solution equilibrium in the direction of the TCO. This kind of reactor, as represented schematically in Figure 14, consequently leads to a very good yield of TCO. After completion of the reaction, which can be monitored by TLC or GC, the pure, final product can be washed out with a mixture of ammonia a methanol[38].

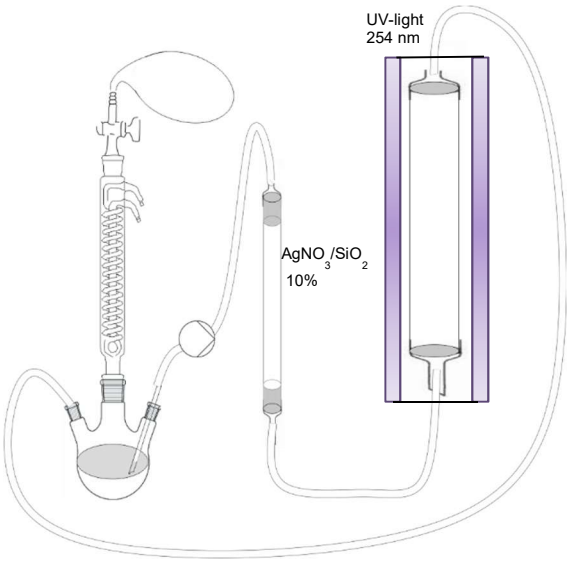

Figure 14: Reactor for TCO synthesis[38]

The next chapter is designed to give a better understanding of the applications of click reactions.

II.5. Imaging

Reactions which can take place in the biosystem are of great interest to the field of biology and chemistry. There are only a handful of bioorthogonal reactions which are already used in many different *in vivo* and *in vitro* applications. The first one to be tested in cellular environment, was a Staudinger ligation between an azide and a phosphine derivate and was reported in 2000 by Bertozzi *et al.*[39]. One year later, a bioorthogonal reaction was used for the first time in an *in vivo* reaction. In this publication, the Staudinger ligation was used for extracellular imaging of tumor cells[40].

Nevertheless, in the last 10 years another reaction with a higher reaction rate and better water compatibility, the so called tetrazine ligation, was brought forth. The first *in vitro* application was shown by Weissleder and his group. They used an addition-reaction between a fluorescent labeled tetrazine and a TCO functionalized protein for extracellular imaging[41]. And finally, Fox and co-workers implemented the first *in vivo* tetrazine ligation for non-invasive pretargeted tumor imaging.[42] Some different imaging methods are illustrated in Figure 15.

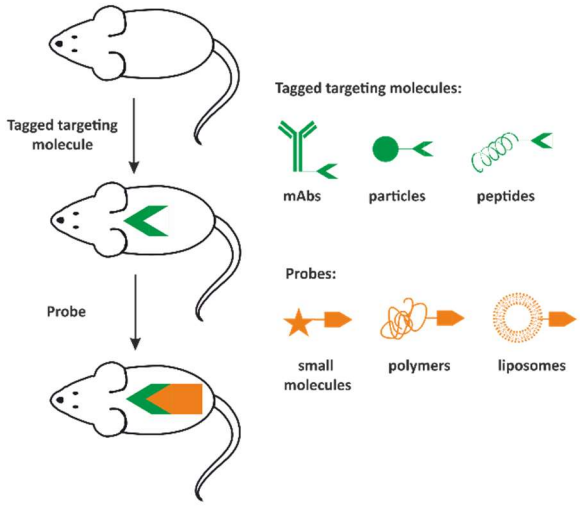

Figure 15: Schematic illustration for in vivo imaging [43]

A short review of the two major imaging methods, which have been described for *in vitro* and *in vivo* imaging in literature, will be given in the next chapter.

II.4.1. Radiolabeling

To get a better overview of biosystems and the mechanism of substances in the human body, visualization of the relevant components such as drugs and proteins, is necessary. One of the most used and developed methods is radiolabeling. 90 % of radiopharmaceuticals are used in the field of diagnostics and only 10 % are used for therapeutics[44].

II.4.1.1.PET

The principle of PET is to use radionuclides with a lower number of neutrons like ^{12}C than the most stable isotope. One of the protons decays to a neutron while emitting positrons. These collide with electrons, lose their mass, and 2 γ-rays are born. The PET scanner has the possibility to scan these γ-rays and to calculate their emitting position[44].

II.4.1.2. Radionuclide

The selection of the right radionuclide depends on the application. The first question that needs to be posed is whether the application is of diagnostic or therapeutic nature. Depending on the answer, radionuclides with high radiation or low radiation are needed[45]. Furthermore, the half-life of the nuclide is an important parameter. This characteristic should be similar to the duration of the biological process being studied[46]. Of course the chemical properties, which are similar to the properties of the most stable isotope[44], the cost, and the availability are of great interest. To summarize, the radioactive dosage should be as low as possible for the patient but as high as necessary. [45][46]

II.4.2 Fluorescent-dye

A very interesting approach to labeling of images are Fluorescent-dyes. The most attractive ones for biological applications are those which are near infrared (650-900 nm) wavelength-excitable. This is due to the fact that many components of biosystems like serum, proteins, haemoglobin, and water have the lowest absorption coefficient between 650 to 900 nm (NIR)[47][48]. A further very important property of biocompatible fluorescent dyes is the water solubility, as already mentioned in chapter II.1.2.1.

II.6. Ibrutinib

Chronic lymphocytic leukemia (CLL)[49] is the most common human haematological malignancy for persons with a median age of 72 in western countries[50]. This is one of three different leukemia diseases next to acute myeloid leukemia (AML)[51] and non-Hodgkin`s lymphoma (NHL)[52], where Bruton's tyrosine kinase (BTK)[53] is expressed. BTK is a non-receptor tyrosine kinase which plays a central role in B-cell development[54], B-cell signaling[55], and B-cell activation[56].

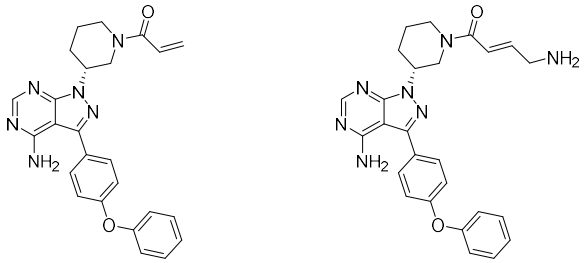

Figure 16: Ibrutinib and a modifiable derivate

One clinically approved BTK inhibitor is ibrutinib (PCI-32756) (Figure 16). To be more precise, the electrophilic group binds covalently to the Cys-481 in the active side, which leads to an irreversible, selective, BTK inhibitor[57].

The next big step in the use of ibrutinib as an intracellular targeting agent, was made by Weissleder and co-workers. They synthesized ibrutinib and modified it with a fluorescent dye to show the potential application as an intracellular imaging agent by covalently binding to BTK[58]. As a proof of concept, they modified the ibrutinib (illustrated in Figure 17) with an amine to get a reactive site and added BODIPY-FL-NHS.

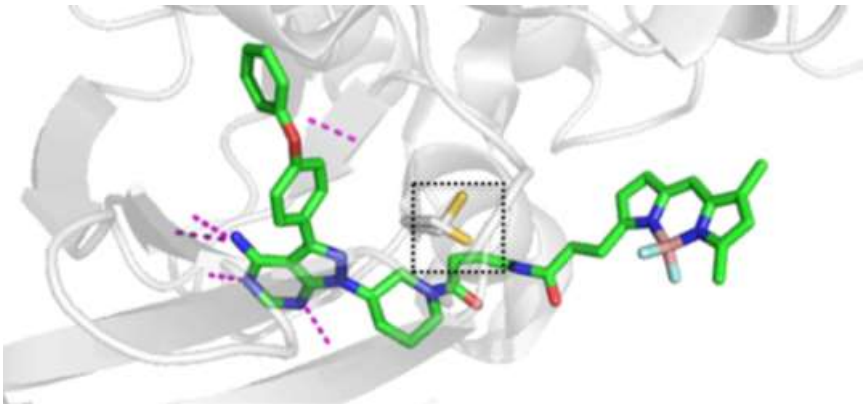

Figure 17: Structure of ibrutinib-BODIPY and its binding positions to BTK[58]

One year later, Weissleder *et al.*[59] published their work on different fluorescent dyes to optimize the model for *in vivo* applications for BTK imaging. The most promising bioconjugate was the ibrutinib SiR-COOH species due to its pharmacokinetic properties and its ability for specific single cell imaging[59].

III. Results and Discussion

III.1. Intracellular Imaging Strategy

As mentioned in the introduction, many different kinds of extracellular targeting agents exist like antibodies, nanoparticles, and peptides. Although other imaging methods are described in literature, the most popular ones utilize these targeting molecules to target the cell. In the subsequent step, an imaging agent like a BODIPY or SIR-COOH fluorescent dye or a radio agent such as ^{18}F is included. These substances react with each other in a bioorthogonal reaction for instance in a copper free click reaction or in a tetrazine ligation and an image of the targeted cell can be acquired, as described in Figure 18[42].

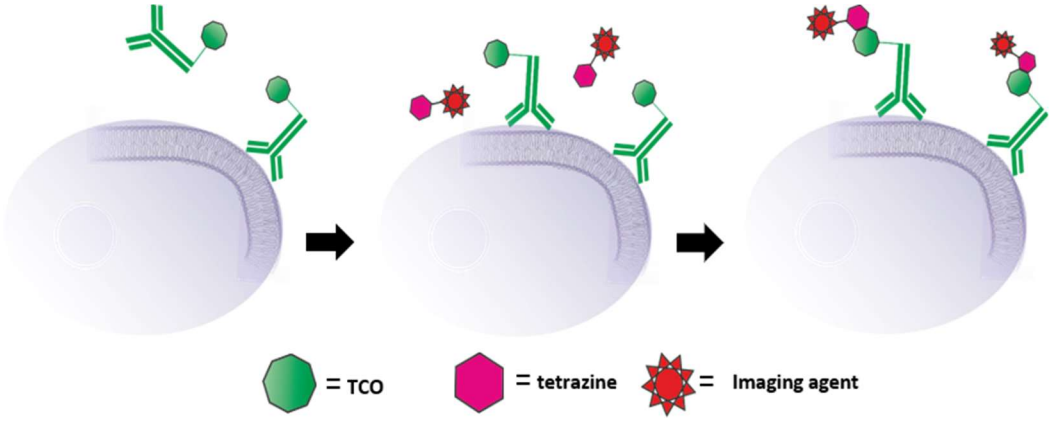

Figure 18: Schematic illustration of extracellular imaging with Antibodies [13]

This is one very promising method for extracellular *in vitro* and *in vivo* imaging. However, in contrast to extracellular imaging, the goal of this work is to find an intracellular targeting and imaging agent and show proof of concept.

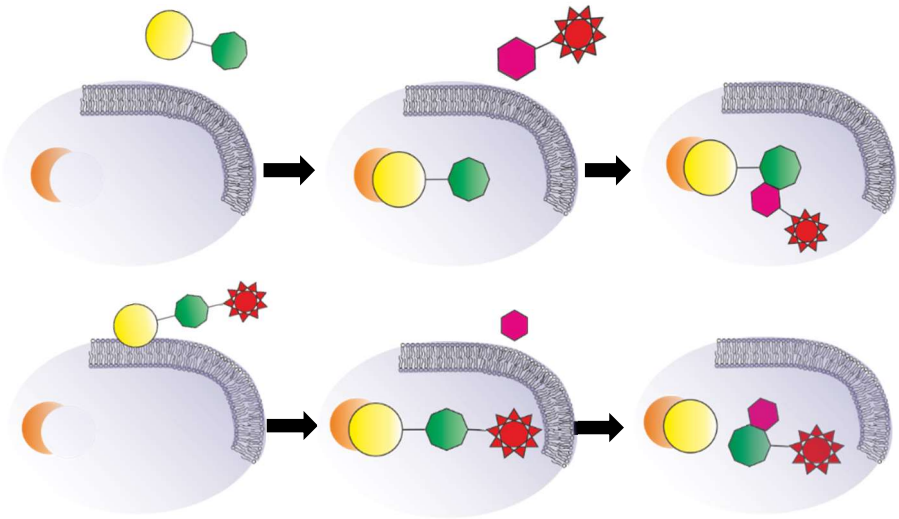

Figure 19: Schematic illustration of intracellular imaging with ibrutinib

Initially, an intracellular targeting agent is needed and the choice falls on ibrutinib. As already described in chapter II.6., ibrutinib binds covalently to BTK and it can be modified without losing its ability to bind to the kinase.[58]

The first possible method, which should be developed, is to use ibrutinib as an intracellular targeting agent. The next question was which kind of reaction to use in order to create a water-soluble bioconjugate with the ability to pass the cell-membrane. Therefore, we decided to use the most biocompatible and fastest already known reaction. This is the click reaction between a TCO and tetrazine, which is linked with the imaging agent as depicted in Figure 19 (top).

There is a reaction which is not very well known for *in vivo* and *in vitro* applications, but which could be very helpful in future applications for double targeting. To explain these, I want to give an example. If we have two different components which are necessary to create the drug (*i.e.* the release product) we can add two different selectivity mechanisms to this drug which leads to a higher specificity in the biosystem. Thus, the first selectivity factor would be ibrutinib and it is absolutely of interest to take a deeper look. The principle is described in Figure 19 (bottom).

III.2. Synthesis Ibrutinib-derivates

The synthesis of ibrutinib[58] starts with a commercially available pyrazolopyrimidine. Through a non-radical iodination with N-iodosuccimidyl, an iodine atom was added on the position 3. The next step was a Suzuki coupling reaction with 4-phenoxybenzen boronic acid. This reaction takes place in the microwave and to reach a high microwave irradiation and temperature of 130 °C, a mixture of dioxolan with water was selected. The precatalyst, palladium-acetate, was activated with the reduction-agent triphenylphosphine to get the active Pd(0)-species.

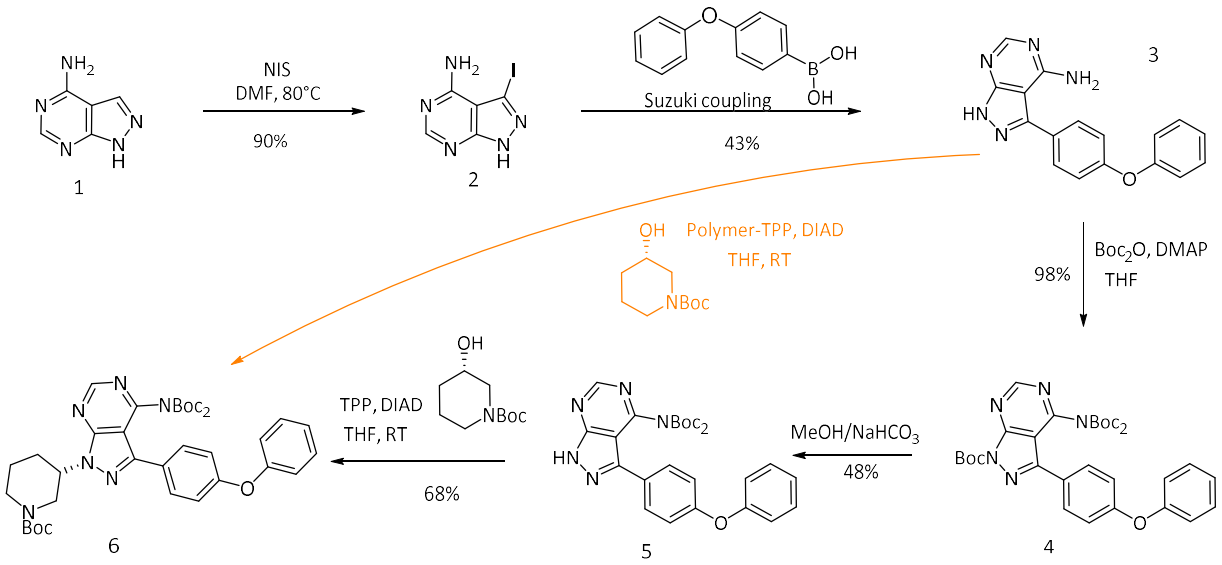

Figure 20: Reaction path for ibrutinib-derivate

In literature, the orange path which you can see in Figure 20 is described. This reaction is a Mitsunobu-reaction; in other words, we have a SN2-mechanism. This kind of reaction preferably takes place under polar aprotic conditions[60]. Therefore, the solvent and other parameters such as temperature and concentration were varied to attain the product. However, product could be found under none of these conditions, neither with TLC nor with LC-MS, due to the bad solubility of compound 3. A result, another synthetic approach was developed.

To manage the solubility problems, the free amine groups were protected with Boc-protecting groups, which leads to a better solubility of **5** in THF. But to get there, **4** has to be treated with a mixture of MeOH/$NaHCO_3$[61]. This results in a slow deprotecting reaction which is quite selective. The requirement to appraise the reaction via TLC remains, as it needs to be stopped after completion of the first deprotecting step. To finalize compound **6**, the Mitsunobu-reaction between **5** and N-Boc-3- hydroxypiperidine works quite well with a good yield.

To reach the amine version of ibrutinib, an acid is necessary. The synthesis route of two different acids are represented in Figure 21. The difference between the two of them is the methyl-group on the amine. This is necessary for the click-to-release reaction, which is explained in chapter II.3.2.1. The starting point for the synthesis of substance **14** is the commercially available 2-(methylamino)ethane-1-ol. First of all, the free amine was protected with Boc to make the Swern oxidation possible, which takes place in the next step. The Swern oxidation is one method to oxidize an alcohol to the aldehyde without over-oxidation to the acid. This was crucial, as the next step is a Wittig reaction. Without this protecting group, the classic Wittig reaction could not take place due to the higher nucleophilicity of an amine compared to an alcohol-group.

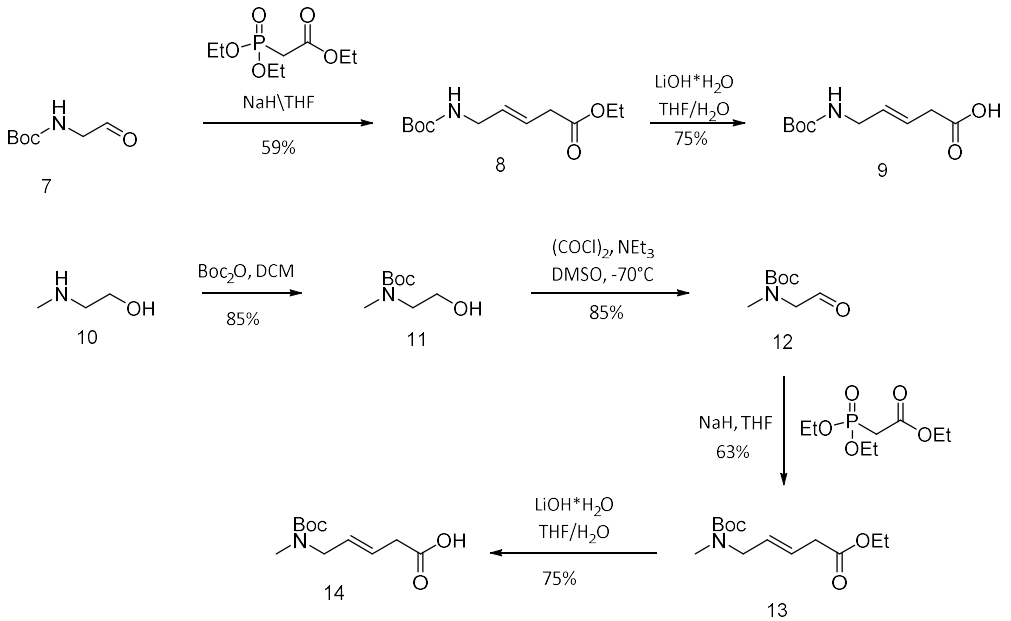

Figure 21: Synthesis of two acids which are needed for the ibrutinib-derivate

The last step is the hydrolysis of the ester to the acid. This carboxyl group is essential for the following coupling reaction between **14** with **6**, and **14** with **9**, due to the mechanism

of the HBTU-coupling reaction. These coupling reactions commence with a TFA catalyst deprotection reaction and are followed by the coupling reaction to get to the final two ibrutinib-derivates Figure 22.

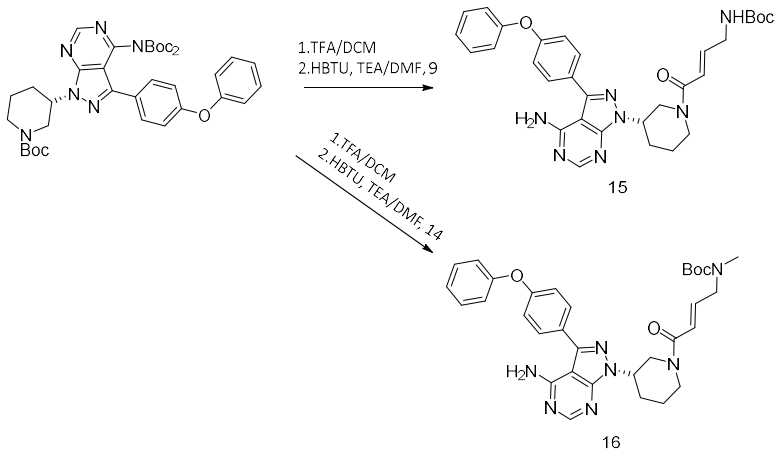

Figure 22: Final step of the ibrutinib-synthesis

III.3. Synthesis and requirements of the TCOs

As already mentioned, two different strategies are considered. The first one is the direct intracellular click reaction and the second one is the click-to-release reaction. Accordingly, different kinds of TCOs were used.

III.3.1 Requirements for the Click Reaction

Two different TCOs were coupled with ibrutinib due to the various abilities of the TCOs. The d-TCO is very fast because of the dioxolan ring, which forces the TCO into a half-chair conformation in distinction to the slower standard crown conformation[25][26]. The dioxolan ring also increases the water solubility. But on the other hand, the standard TCO is well known in literature and very stable in biosystems, which we are not able to claim for the d-TCO (Figure 23).

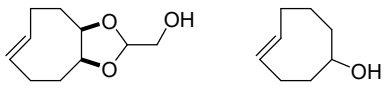

Figure 23: Structure d-TCO and standard TCO

III.3.2 Requirements for Click-to-release Reaction

In contrast to the standard click reaction, for the click-to-release reaction, a multifunctional TCO (Figure 24) is necessary. To get the release ability, one of the moieties has to be in allylic position. On the one hand the position of second functionality is irreversible, on the other hand it will serve as arm for the targeting agent. A further important characteristic for a good release TCO is the regioselectivity of the two different moieties. Therefore, a methyl group

was introduced on the position 4. The sterical effect of this methyl group is strong enough to cause a difference in reactivity between the ester- and carbonate group. Furthermore, two leaving groups were added on the moieties, which enables a nucleophilic attack for the following coupling synthesis.

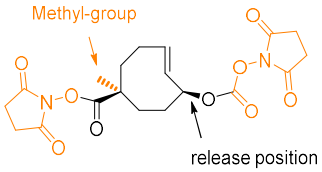

Figure 24: m-TCO-bis-NHS

Beside the basic requirements mentioned above, one more is noteworthy. As a consequence of the two moieties, four different diastereomers can be formed if more than one diastereomer is used for isomerization. To prevent this, a synthesis was chosen which leads to only one diastereomer. Furthermore, the axial and equatorial products which occur through the isomerization can be separated quite easily due to the fact that one isomer hydrolyses rapidly. This fact will be explained in detail in the following chapter.

III.3.3 Synthesis m-TCO

The synthesis of m-TCO-bis-NHS-ester was commenced with a very cheap commercially available 1,5-cyclooctadien. The electrophilic addition of hydrobromic acid was followed by removal of the byproduct, dibromcyclooctane, via distillation.

Compound **18** was prepared via nucleophilic substitution of the bromide with cyanide. However, this reaction has one disadvantage. As already known, good solvents for a nucleophilic reaction are aprotic but very polar[60]. Therefore, this reaction is carried out in DMSO, which has high carrier abilities for substances through the skin barrier. As result, the combination with the highly toxic NaCN makes the reaction lethal if it comes into contact with the skin.

This step was followed by a hydrolysis reaction of the nitrile to the COOH group and was accelerated through dihydrogenperoxide due to the peroxide-intermediate which occurs[62] (Figure 25).

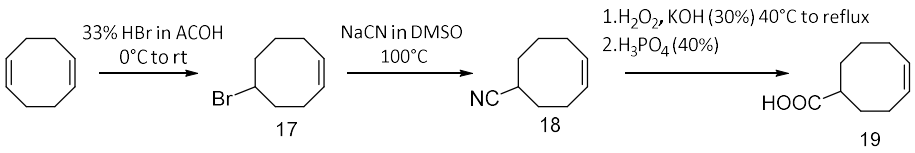

Figure 25: First steps m-TCO synthesis

The following steps commencing from compound 19 until the m-TCO-bis-NHS-ester, were designed by Rossin *et al.* and are illustrated in Figure 26 [29]. The reaction begins by adding a methyl-group on position 1. To do this, a strong base, in this case LDA, for deprotonation of the hydrogen-atom from the carboxylic acid and from position 1, was used.

The subsequent iodolactonization was carried out in a two-phase system of DCM and alkaline water. To get a water-soluble iodine species, potassium iodine was added. Through the first deprotonating step, compound **18** transferred into the aqueous-phase where the iodine atom forms a three-ring intermediate with the double bond. This electrophile can be attacked by the intermolecular nucleophile center to form the most stable 6 membered-ring. Furthermore, this nucleophilic ring-closing follows a stereospecific backside-attack. Afterwards, the product goes back to the organic phase, where a stereospecific product can be isolated.

To reach component **23**, the following steps are necessary. The first one is an elimination reaction with $KHCO_3$ in MeOH and afterwards a ring-opening reaction with DBU was chosen. This reaction leads to a diastereomer-pure product with two moieties.

The next step is the forming of a TCO out of the *cis*-Cyclooctene. As described in chapter II.4 this reaction is photosensitive and leads to the axial and equatorial products. In most cases, the separation of these two products is very difficult and time-consuming. But according to Rosin *et al.*[28], the following ester hydrolysis has different reaction kinetics depending on spatial position of the ester group. Therefore, after the following reaction the product is again diastereomer-pure.

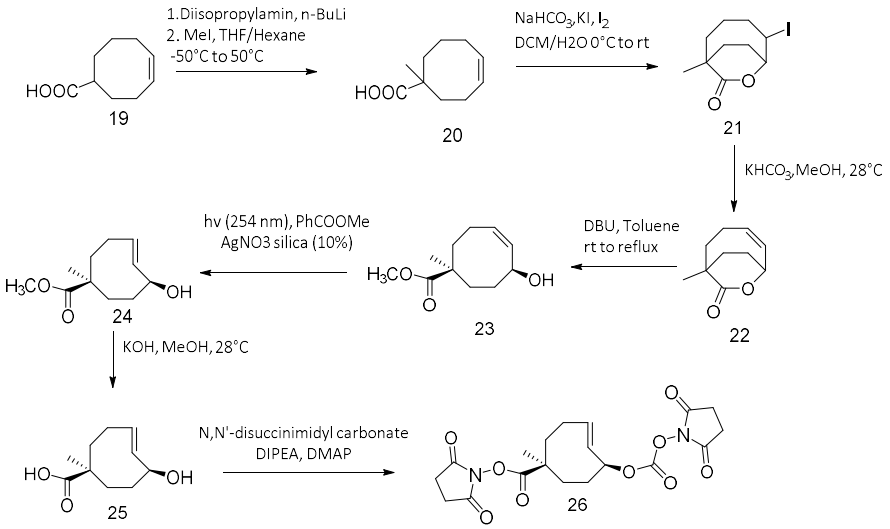

Figure 26: m-TCO Synthesis [28]

The only downside to the synthesis from m-TCO-bis-NHS-ester is the last step by adding good leaving groups on both functionalities. In literature, a low stability of the product is described, which can be the reason for the low yield. Therefore, a catalyst for nucleophile reactions (4-dimethylaminopyridine) was added[28].

III.4. Testing Components

The idea behind this thesis is to show that chemical reactions can take place intracellularly. As proof of concept, ibrutinib was designed as an intracellular targeting agent and therefore constitutes the central part of every component, which was tested. It was modified with TCOs and linker (*e.g.* PEG) to increase the biocompatibility of the components.

The two most common TCOs for *in vivo* applications are the standard TCO, due to its biocompatibility, and the d-TCO, due to better water solubility in comparison to standard-TCO and the high reaction rate. Therefore, these components are ideal for the first model of designing an intracellular click-reaction. On the basis of two different reasons we decided to add a PEG_6-linker between the other components. This linker has the ability to make the bioconjugate more water-soluble and biocompatible. Furthermore, the distance between the TCO and the enzyme becomes larger. This means that the click reaction between the tetrazine and the TCO is less sterically hindered. But on the other hand the substance becomes more polar and therefore it is not as good at passing through the cell-membrane[63]. The chemical structure of the bioconjugates are illustrated in Figure 27.

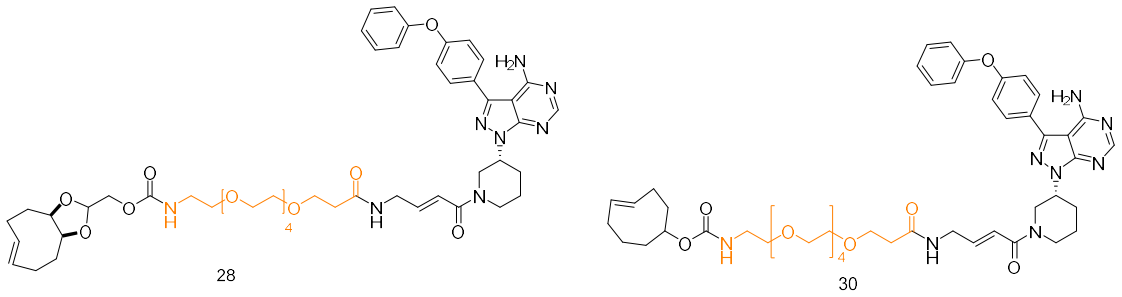

Figure 27: Testing compounds for the intracellular click reaction

The straight forward reaction has a TCO modified with a good leaving group as a starting point: d-TCO-PNP-Ester and standard-TCO-NHS-ester. The latter was coupled with the PEG_6-Linker, which in turn was coupled with ibrutinib to get the final components **28** and **30**. For the second reaction, HBTU was used as coupling reagent. HBTU is commonly used for making peptide-bonds by adding a leaving group on the acid in the first step and afterwards the nucleophile can attack the electrophile to form the peptide-bond.

Besides the addition reaction, the click-to-release reaction should be tested intracellularly as well. Therefore, the central point of the bioconjugate is the m-TCO. The latter is equipped with an ester and carbonate functionality. Based on the electronic effect, the ester moiety should be more electrophilic. Nevertheless, through the steric shielding of the methyl group, the reactivity of this side is lower. Thus, the first step is to add ibrutinib on the release side. In this case, the ibrutinib derivate with the methyl group was used. This methyl-group plays a critical role for a better release due to the fact that no intramolecular attack can take place and the yield of the release reaction becomes higher[33]. Thus, this reaction starts with the deprotecting reaction of the ibrutinib derivate and afterwards a coupling reaction on the release side of the m-TCO is implemented. This component **33** is not stable, necessitating the direct conversion with ethylenediamine to get to substance **34**.

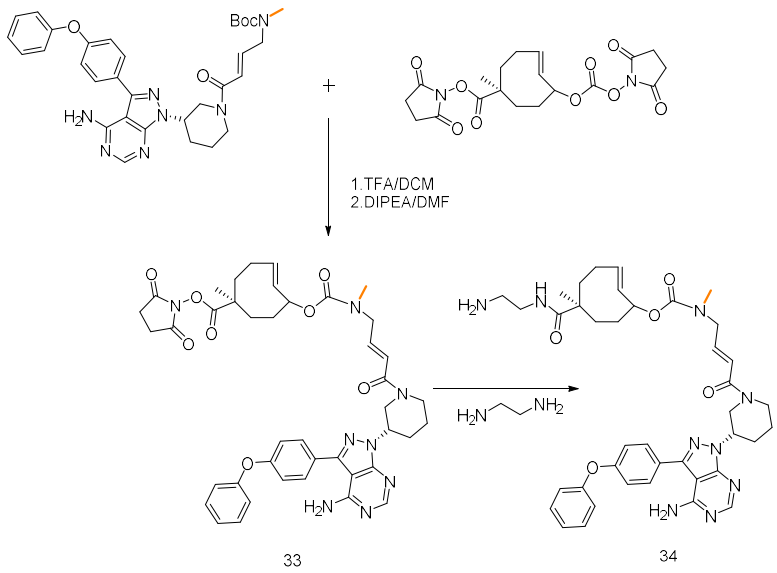

Figure 28: Coupling reaction of m-TCO with ibrutinib

To visualize the reaction at very low concentrations, similar to concentrations which would occur in biosystems, a fluorescent dye with a high extinction coefficient needs to be utilized. Therefore, and on the basis of the good water-solubility compared to other dyes, Sir-COOH-dye with an extinction coefficient of ~100 000 $M^{-1}cm^{-1}$ [64] was chosen.

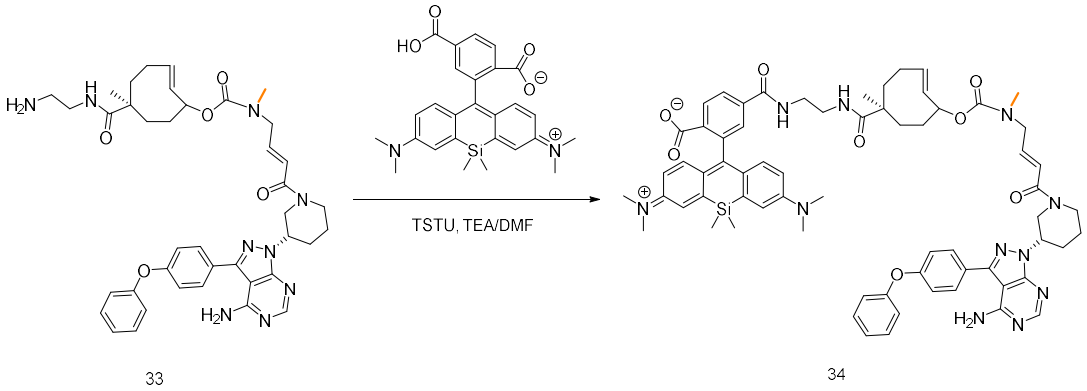

Figure 29: Final step for the m-TCO-ibrutinib-SIR species

The reaction, which is illustrated in Figure 29, is a coupling reaction with TSTU. Hence, all components for the following *in vitro* test have been synthesized. To get a preliminary click-to-release result, this reaction was tested and monitored with LC-MS, which will be discussed in the following chapter.

III.5 Click-to-release Measurement

With the goal of pinpointing the release of the ibrutinib-derivate, a low concentration (100 µM) measurement in PBS buffer (pH=6.8) was performed with the m-TCO-Sir-ibrutinib-species. The reaction was screened after 1 h, 3 h, 9 h, 21 h and one further measurement was taken after 24 h to show that the endpoint of the reaction had been reached. To visualize the results, the reaction-mixture was directly incubated into the LC-MS (10-100% acetonitrile in water; 5 min 1.5 ml/min) and analyzed with a UV-detector combined with MS. The

fluorophore, SIR-dye, which has is absorption maxima at the wavelength of 650 nm, enabled the characterization of the reactant and of one of the products.

The second reaction compound was 3,6-dimethyl-1,2,4,5-tetrazine, with a concentration of 150 µM, to allow comparison with results in literature. Furthermore, the concentration of DMSO was 5%.

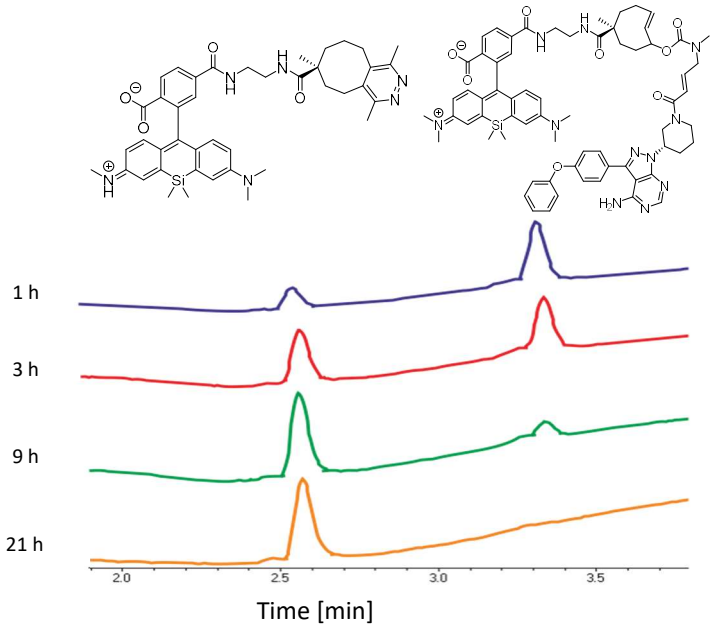

Figure 30: Results for the click-to-release measurement

Considering the UV-chromatogram displayed in Figure 30, two peaks could be assigned to the corresponding m/z values and products which should occur due to the mechanism. No side-product could be found, and the reaction yield is 90 % when normalizing the integral Sir-product to the starting compound. One further m/z-Value could be identified and allocated to the release-product, the ibrutinib derivate.

As a result, the introduction of the methyl group worked quite well and leads to the desired results, which means no intermolecular attack could be observed and the reaction was finished after 21 h with a pH-value comparable to the pH-value in human bodies. Nevertheless, this reaction has to be tested *in vitro* and afterwards *in vivo* as well to make a statement concerning the biocompatibility.

III.6 *In Vitro* Testing

Initial information about biocompatibility and the effect of the substance to biosystems was generated with *in vitro* tests. To that end, HT1080 fibrosarcoma cells where cultured in well plates. In addition to the blind sample row, where no cells were cultured, two different aspects were compared to each other. In 50 % of the samples, fetal bovine serum (FBS) was added to imitate the environment in the blood. This enables the study of protein binding or shielding effects of the bioconjugates, which could lead to worse cell-permeability or to trapping of the bioconjugate. There was, however, no significant difference between the result with or without FBS.

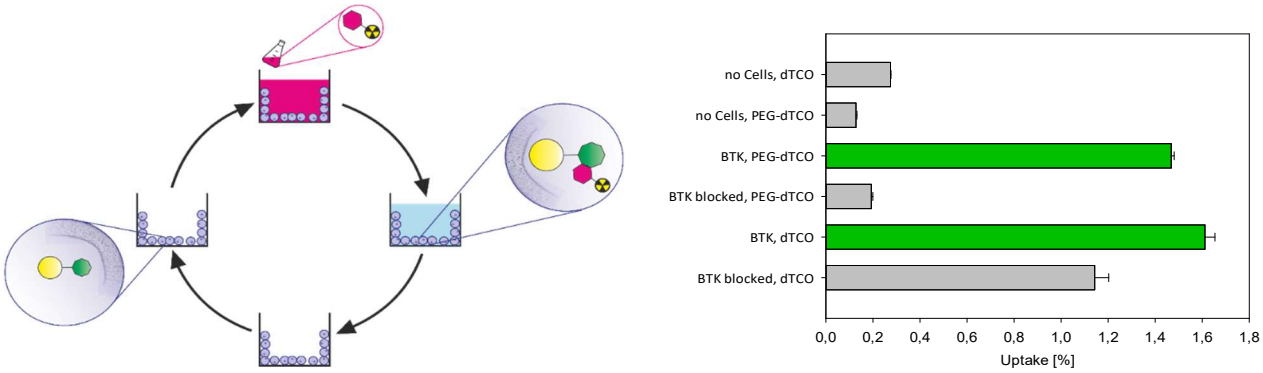

Figure 31: left: Scheme for imaging with radiolabeled tetrazines; right: results for in vitro click reactions

Furthermore, two different species were explored to show their binding and clicking behavior. The first compound was a d-TCO-ibrutinib-species and in the second one, PEG_6 was introduced as linker between the d-TCO and ibrutinib.

The reasons for this are versatile. Primarily, the higher hydrophilicity due to the PEG-group causes better solubility in the blood and faster distribution in the body with the downside of worse cell-permeability. Furthermore, the distance between the BTK, the enzyme to which ibrutinib binds covalently, and the d-TCO is higher due to the PEG_6 -group. These could have the consequence that the d-TCO is less sterically hindered and the click reaction could lead to a higher yield.

In addition, one row of samples with HT1080 fibrosarcoma cells were blocked, which means that these cells were incubated for 120 min with the pure ibrutinib-derivate. This has the consequence that the BTK is already blocked and the testing species cannot bind to BTK. Therefore, a comparative sample has been designed to which all other values can be normalized.

In this case, analytics consisted of a radiolabeled tetrazine, which is illustrated in Figure 32. The tetrazine was synthesized through a copper catalyzed reaction.

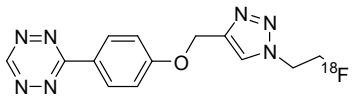

Figure 32: Radiolabeled tetrazine

After cultivation of the cells and incubation of the blocked cells, the ibrutinib-species was added to the cells and incubated for 120 min, ensuring that all of the ibrutinib can bind to BTK. Afterwards, the wells were washed three times to remove remaining ibrutinib. Ultimately, the freshly synthesized radiolabeled tetrazine was incubated with the cells to click with the d-TCO intracellularly. After 90 min reaction-time, the wells were washed three times, the cells were dissociated from the wells and injected into the gamma-counter to determine the rest-concentration of the F^{18}-atoms.

As show in Figure 31, the d-TCO-ibrutinib as well as the d-TCO-PEG-ibrutinib-species result in a high amount of radiolabeled substance. The only significant distinction is between the blocked species. If the d-TCO-compound without PEG is used for the blocked cell, the uptake is similar to the one without cells, which is in accordance with expectations. The compound without PEG, however, shows a high uptake if it is incubated with the blocked cells. The only logical reason which could explain this phenomenon, is that the PEG-species has a

higher specificity to BTK than the compound without PEG. The inversion of the argument, namely that the d-TCO-ibrutinib species binds or gets trapped somewhere in the cell or on the surface, could equally hold. These effects can occur as well when using the non-blocked cells and therefore, the end results need to be normalized to the blocked-values. Taking this into account, the PEG-species shows better results.

IV. Conclusion and Outlook

First of all, two different modifiable ibrutinib- derivates were successfully synthesized. These intracellular targeting agents were modified with different TCOs (standard TCO, d-TCO, m-TCO) to develop bioconjugates with distinct abilities.

The most promising candidate for the intracellular click reaction is the d-TCO compound. Especially the species with a PEG_6-linker between the d-TCO and the ibrutinib shows magnificent results while testing in HT1080 fibrosarcoma cells as the intracellular click reaction takes place. To complement this analysis, investigation *in vivo* is necessary and therefore testing in mice is currently being undertaken. For that purpose, a standard-TCO with ibrutinib was synthesized again with the PEG_6-linker due to the results of the *in vitro* results. The big advantage of the standard-TCO is its documented high *in vivo* stability, which has not been stated about the d-TCO. For the first *in vivo* reactions, which were done in our research group, this component was used and shows confident results.

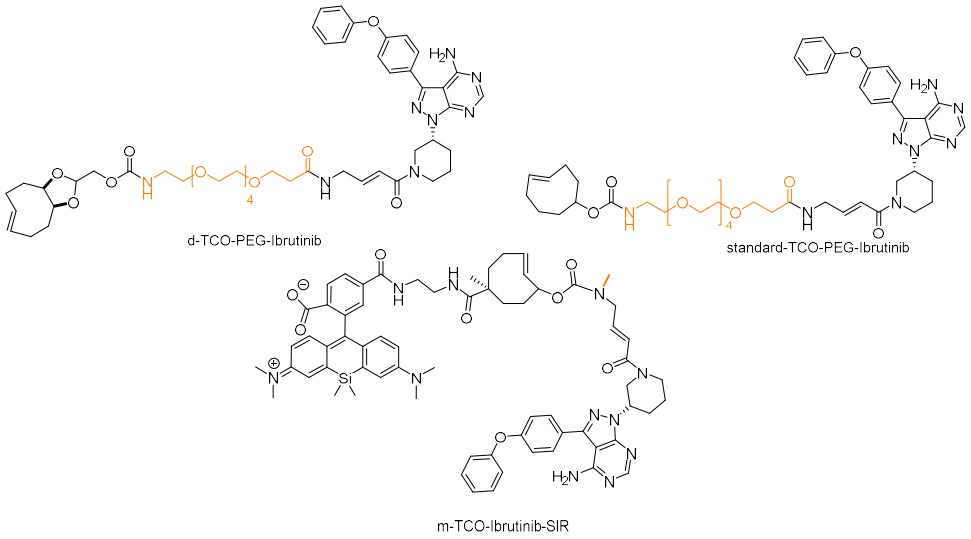

Figure 33: Species for the click reaction (top), click-to-release bioconjugate (bottom)

The second part is the more challenging click-to-release reaction. As mentioned previously, the ibrutinib derivate with a methyl-group on the amine was synthesized for a better release as described in chapter II.3.2.1. This prediction was confirmed trough the LC-MS measurement of the click-to-release reaction of an m-TCO-ibrutinib-SIR-species. In this measurement, no side-product was found. This means that the intermolecular attack of the amine, which would lead to a dead-end, cannot occur. Furthermore, after 21 hours, the reactant was completely converted. Of course, this species should be tested *in vitro* for insight into the intracellular-binding mechanism of this ibrutinib-species to BTK and to reveal if the click-to-release reaction can occur intracellularly. Testing in mice is necessary to attain information about *in vivo* stability of the component as well as about the binding mechanism and the click-to-release reaction for *in vivo* applications. Hopefully, this will be a small step in the direction of fighting cancer and other diseases.

V. Experimental Part

V.1.Chromatography

V.1.1 Thin Layer Chromatography

Thin layer chromatography (TLC) was carried out on TLC-aluminum sheets (Merck, silica gel 60 F_{254} or silica gel 60 RP-C18 $F_{254}S$ for very polar compounds). Visualization of the spots was achieved either by UV irradiation (254 or 366 nm) or by heat staining with ceric ammonium molybdate in ethanol/sulfuric acid.

V.2.2 Column Chromatography

Flash chromatography and preparative liquid chromatography (Prep LC) was carried out, if not mentioned otherwise, on a Grace Reveleris® PREP Purification System. The Reveleris® PREP Purification System is a computer controlled integrated system (Figure 34).

The corresponding PP cartridges and glass columns for flash chromatography were packed with silica gel 60 (Merck, 40-63 µm). For Prep LC two different columns were used:

- Phenomenex Luna 10µm, C18, 100 Å, 250 x 10 mm
- Phenomenex Luna 10µm, C18, 100 Å, 250 x 21 mm

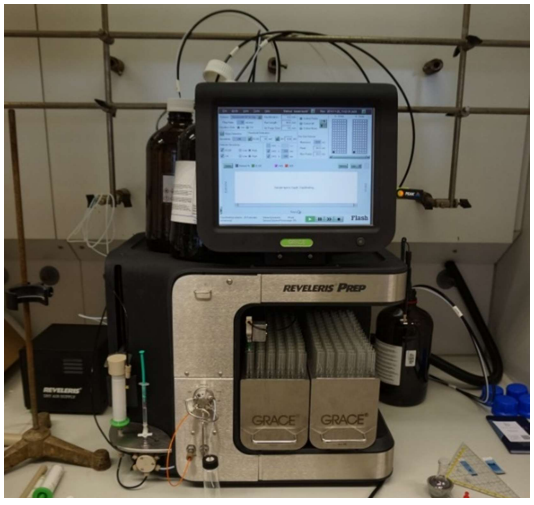

Figure 34 Grace Reveleris® PREP Purification System:

The compositions of the mobile phase as well as the amount of silica gel respectively the type of the used columns (Prep LC) are mentioned in the respective synthesis.

V.2. Analysis

V. a. 3.1. GC/MS

GC/MS experiments were done with a Thermo Finnigan GC 8000 Top gas chromatograph on a BGB5 column (l=30 m, di=0,32 mm, 1 µm coating thickness) coupled to a Voyager quadrupole mass spectrometer (electron ionization, 70 eV). GC-FID were measured on a Thermo Scientific Focus GC with FID detector, Triplus auto sampler and BGB5 column.

V. a. 3.2. LC/MS

LC-MS measurements were carried out on a HPLC system of Agilent Technologies with the following components:
Agilent 1200 Series G1367B HiP ALS Autosampler
Agilent 1100 Series G1311A Quat Pump
Agilent 1100 Series G1379A Degasser
Agilent 1200 Series G1316B TCCSL
An Agilent 1260 Infinity G1315D DAD as well as an Esquire HCT Ion Trap MS of Bruker served as detectors.

V. a. 3.3. NMR

NMR spectra were recorded at a Bruker DPX-200 as well as an Avance DRX-400 Fourier transform-spectrometer. The chemical shifts are referred to trimehtylsilane and are represented in ppm. For calibration, solvent signals were used. The multiplicities of the peaks are abbreviated as follows:
^{1}H: singlet (s), broad signal (bs), doublet (d), triplet (t), quadruplet (q) and multiplet (m); ^{13}C: quaternary C (q), CH (p), CH_2 (s), CH_3 (t) (assignment from APT-experiments).

V.3. Synthesis and Characterization of Substances

V.3.1. 3-iodo-1H-pyrazolo[3,4-d]pyrimidin-4-amine

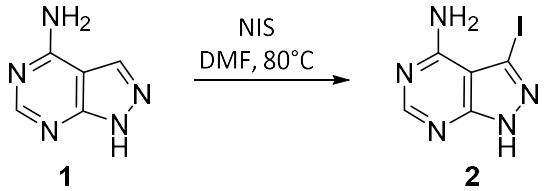

Substances	equivalent	n [mmol]	M [g/mol]	m /V
1	1	29.6	135.16	4 g
NIS	1.5	44.4	224.98	10 g
DMF				24 ml

Procedure:

1 and NIS were filled into a flask with septum and were purged with Argon. Afterwards, DMF was injected through the Septum and heated to 85°C to get a clear solution. After 30 min, the colorless solution turned into a brown-black solution. The reaction mixture then was stirred at 80°C overnight. The resulting dark brown suspension was filtered and washed with water (2x 20 mL), methanol (3x 20ml) and Et_2O (1x20 ml). The solvent was removed in vacuo, revealing a white solid.

Yield: 4.2 g white solid (54% of theory)

Analysis:

R_f(DCM:Methanol 10:1): 0,63

H-NMR**:** ^{1}H NMR (400 MHz, DMSO-d_6) δ 13.79 (s, 1H), 8.16 (s, 1H), 3.33 (s, 2H).

V.3.2. 3-(4-phenoxyphenyl)-1H-pyrazolo[3,4-d]pyrimidin-4-amine

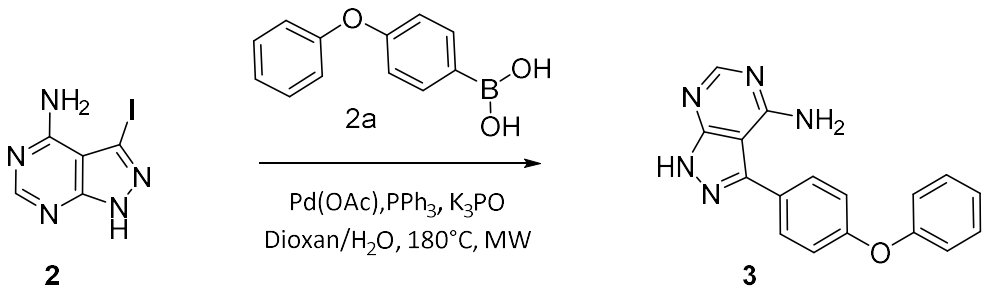

Substances	equivalent	n [mmol]	M [g/mol]	m /V
2	1	3.8	261.03	1 g
2a	2	7.7	214.03	1.64 g
K_3PO_4	3	11.5	212.28	2.44 g
$Pd(OAC)_2$	0.25	0.96	224.51	0.215 g
PPH_3	2	7.7	262.28	2.01 g
Dioxane/H_2O (1:4)				15 ml

Procedure:

A microwave-vial with magnetic stirrer was charged with **2**, **2a**, K_3PO_4, $Pd(OAc)_2$, PPH_3, and a mixture of water/dioxane (4:1). The resulting suspension was then degassed by argon bubbling for 20 min and finally the reaction took place in the microwave at 130°C with a pressure of 2 bar for 1 h. The resulting sponge-like yellow solid was dissolved in 600 ml EE and was washed 3 times with 200 ml H2O. This aqueous phase was again washed once with EE. The organic phases were combined and dried over Na_2SO_4. This drying agent was removed via filtration and the solvent was evaporated via vacuum distillation. The precipitate was suspended in DCM and finally the solid was separated from the solution via filtration.

Yield: 1.4 g (60% of theory)

Analysis:

R_f(DCM:Methanol 10:1): 0.98

H-NMR: ^{1}H NMR (400 MHz, DMSO-d_6) δ 13.48 (s, 1H), 8.14 (s, 1H), 7.59 (d, *J* = 8.2 Hz, 2H), 7.36 (t, *J* = 7.8 Hz, 2H), 7.22 – 7.08 (m, 5H), 6.73 (s, 2H).

V.3.3. tert-butyl 4-((di(tert-butoxycarbonyl))amino)-3-(4-phenoxyphenyl)-1H-pyrazolo[3,4-d]pyrimidine-1-carboxylate

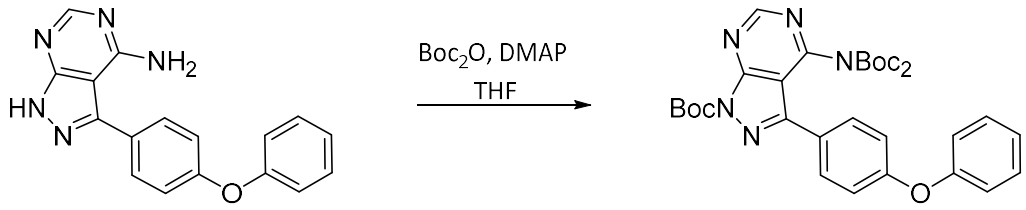

3 **4**

Substances	equivalent	n [mmol]	M [g/mol]	m /V
3	1	9.4	303.33	2.85 g
BOC_2O	4	37.6	218.25	8.20 g/ 8.4 ml
DMAP	0.33	3.1	112.17	0.35 g
THF				105 ml

Procedure:

A flask was filled with **3** and DMAP, flushed with argon and afterwards absolute THF was added trough a septum, which lead to formation of a white suspension. After the Boc_2O was added drop by drop, the result was a brown-green solution which was stirred overnight. Afterwards, the solvent was removed by rotary evaporation. The residue was dissolved in EE and washed three times with 1 N HCl and once with brine. This organic phase was dried over Na_2SO_4, filtrated, and the solvent was removed in vacuum.

Yield: 5.3 g (93.5% of theory)

Analysis:

R_f (PE:EE 3:1): 0,625

H-NMR: ^{1}H NMR (400 MHz, Chloroform-*d*) δ 9.15 (s, 1H), 7.74 (d, *J* = 8.7 Hz, 2H), 7.38 (dd, *J* = 8.6, 7.4 Hz, 2H), 7.19 – 7.13 (m, 1H), 7.12 – 7.02 (m, 4H), 1.74 (s, 9H), 1.29 (s, 18H)

V.3.4. tert-butyl 4-((di(tert-butoxycarbonyl))amino)-3-(4-phenoxyphenyl)-1H-pyrazolo[3,4-d]pyrimidine-1-carboxylate

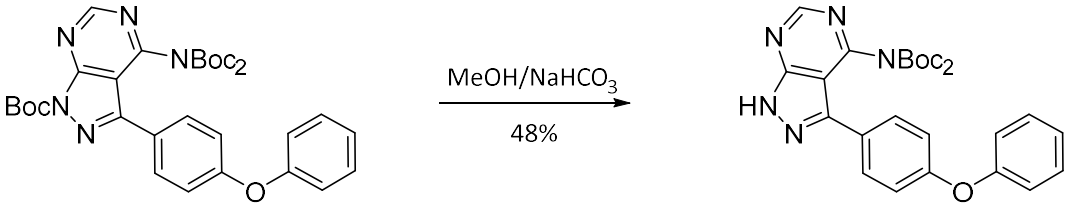

4 **5**

Substances	equivalent	n [mmol]	M [g/mol]	m /V
4		8.79	603.28	5.3 g
MeOH				84 ml
$NaHCO_3$				39.2 ml

Procedure:

Compound **4** in anhydrous MeOH was degassed by argon bubbling. Then a saturated $NaHCO_3$-solution was added. Subsequently, the mixture was heated to 50°C and every 10 min a TLC was made to determine the conversion of the reaction. After conclusion of the reaction, according to TLC, the product was extracted with EE (3x100 ml) and then washed with 2 N HCl (2x 100 ml) and brine (1x 100ml). Then, the combined organic extracts were dried, concentrated, and purified by column chromatography (200 g silica, 10 – 50 % in 50 min 50->100% in 10 min EE in PE).

Yield: 3.8 g white-yellow powder (86% of theory)

Analysis:

R_f (PE:EE 2:1): 0.4

H-NMR: ^{1}H NMR (400 MHz, Chloroform-*d*) δ 9.00 (s, 1H), 7.73 (d, *J* = 8.8 Hz, 2H), 7.39 (dd, *J* = 8.6, 7.4 Hz, 2H), 7.18 (t, *J* = 1.1 Hz, 1H), 7.13 – 7.03 (m, 4H), 1.31 (s, 17H).

V.3.5. (R)-tert-butyl 3-(4-((di(tert-butoxycarbonyl))amino-3-(4-phenoxyphenyl)-1H-pyrazolo[3,4-d]pyrimidin-1-yl)piperidine-1-carboxylate

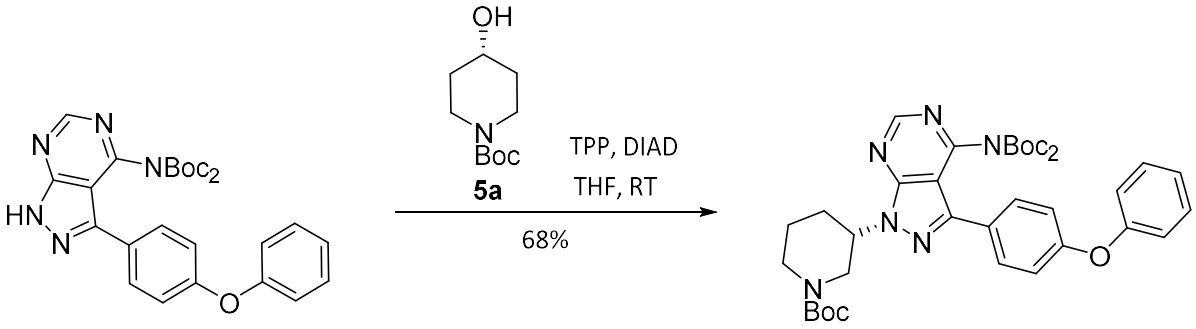

5 **6**

Substances	equivalent	n [mmol]	M [g/mol]	m /V
5	1	5.96	503.22	3 g
5a	2	12	201.14	2.41 g
TPP	2	12	262.29	3.15 g
DIAD	2	12	174.15	20.9 g

Procedure:

5, **5a**, and TPP were filled into a flask and purged with argon. 200 ml of absolute THF (inhibitor free) was added through a septum. The next step was to add DEAD drop-wise while the solution was cooled. The solution changed color from colorless to yellow while it stirred overnight. Then, the solvent was evaporated in vacuum and the residue dissolved in 200 ml EE to wash it with saturated NH_4Cl-solution (3x100ml). The organic phase was dried over NaSO4, the solvent removed in vacuum and liquid chromatography was carried out (2x90g SiO_2 5→50 in 40 min 50→100 in 10 min EE:PE) .

Yield:

Crude: 3.8 g

1 g, after chromatography: 0.65 g (60.4% of theory)

Analysis:

R_f (PE:EE 2:1): 0.78

H-NMR: ^{1}H NMR (400 MHz, Chloroform-*d*) δ 8.92 (s, 1H), 7.69 (d, *J* = 8.8 Hz, 2H), 7.38 (dd, *J* = 8.6, 7.4 Hz, 2H), 7.20 – 7.11 (m, 1H), 7.13 – 7.01 (m, 4H), 4.96 (dt, *J* = 11.0, 6.2 Hz, 1H), 4.35 (s, 1H), 4.16 (td, *J* = 13.5, 7.3 Hz, 1H), 3.47 (d, *J* = 16.2 Hz, 1H), 2.86 (t, *J* = 12.8 Hz, 1H), 2.35 – 2.17 (m, 3H), 1.92 (d, *J* = 13.6 Hz, 1H), 1.78 – 1.66 (m, 1H), 1.32 (s, 24H).

V.3.6. (E)-ethyl 4-((tert-butoxycarbonyl)amino)but-2-enoate

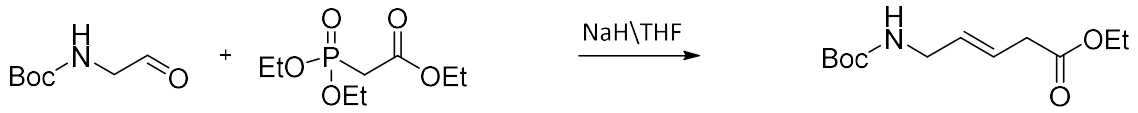

7 **7a** **8**

Substances	equivalent	n [mmol]	M [g/mol]	m /V
7	1	5.97	159.18	0.95 g
7a	2.34	13.97	224.19	3.13 g/ 2.77 ml
NaH	2	11.94	23.99	0.477 g

Procedure:

NaH was filled into a 3-neck-flask and purged with argon. Then, 30 ml of absolute THF was added and stirred for around 10 min until the complete NaH was dissolved. The next step was to cool the solution to 0°C and **7a** was added drop-wise over 20 min. Afterwards, the cooling bath was removed and **7**, which was dissolved in 10 ml THF, was injected drop by drop over 15 min. This lead to a bright yellow solution. After 30 min, TLC showed complete conversion and therefore the solution was diluted with 30 ml of H_2O. This mixture was washed with EE (5x 50 ml), the organic phase was dried over Na_2SO_4 and the solvent was removed in vacuum. The final purification took place with liquid chromatography (90 g SiO2 10→50 in 25 min 50→100 in 5min)

Yield: 0.7 g (41% of theory)

Analysis:

R_f (PE:EE 1:1): 0.72

H-NMR: ^{1}H NMR (400 MHz, Chloroform-*d*) δ 6.88 (t, *J* = 4.9 Hz, 1H), 5.95 (t, *J* = 1.9 Hz, 1H), 4.70 (s, 1H), 4.19 (d, *J* = 7.1 Hz, 2H), 3.92 (s, 2H), 1.45 (s, 10H), 1.28 (t, *J* = 7.1 Hz, 3H).

V.3.7. (E)-4-((tert-butoxycarbonyl)amino)but-2-enoic acid

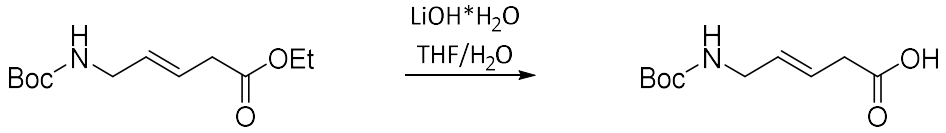

8 **9**

Substances	equivalent	n [mmol]	M [g/mol]	m /V
8	1	2.97	229.13	0.68 g
LiOH*H$_2$O	5	14.84	41.96	0.62 g

Procedure:

A flask was charged with 20 ml absolute THF, **8**, and bubbled with Argon. LiOHxH$_2$O was dissolved in 13 ml H$_2$O and injected into the solution trough a syringe. The reaction took place overnight. THF was evaporated and the resulting yellow aqueous solution was acidified with 1 N HCl to pH 3 and extracted with EE (4x 30 ml). This washing process was repeated one more time and the combined organic phase was dried over Na$_2$SO$_4$. The work-up was concluded by a chromatography step (SiO2 8g 0→15% in 30 min 15→15% for 30 min DCM:Methanol)

Yield: 0.3 g (50,2% of theory)

Analysis:

R$_f$ (DCM:Methanol 10:1): 0.3

H-NMR: ^{1}H NMR (400 MHz, Chloroform-*d*) δ 10.12 (s, 1H), 6.87 (d, *J* = 15.5 Hz, 1H), 5.88 (d, *J* = 15.5 Hz, 1H), 5.18 (s, 1H), 3.86 (s, 2H), 1.43 (s, 10H).

V.3.8. Tert-butyl(2-hydroxyethyl)(methyl)carbamate

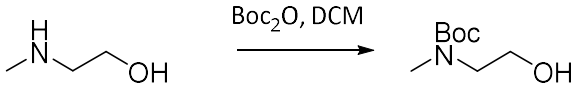

10 **11**

Substances	equivalent	n [mmol]	M [g/mol]	m /V
10	1	13.3	75.07	1 g
Boc_2O	1	13.3	218.3	2.9 g
DCM				30 ml

Procedure:

A three-neck-flask with dropping funnel and argon balloon was charged with **10** and cooled with an ice bath. Through the dropping funnel Boc_2O, which was dissolved in 30 ml DCM, was added drop by drop. This mixture was stirred over the weekend at room-temperature and afterwards concentrated in vacuo at 40 °C. The crude residue was dissolved in brine, extracted four times with 50 ml EE, washed again with brine and this aqueous phase was extracted again thrice with EE. The combined organic phases were dried over Na_2SO_4. The filtrate was evaporated to attain the final product.

Yield: 2.1 g (90% of theory)

Analysis:

R_f (pure EE): 0.71

H-NMR: ^{1}H NMR (200 MHz, Chloroform-*d*) δ 3.70 (t, *J* = 5.4 Hz, 2H), 3.35 (t, *J* = 5.4 Hz, 2H), 2.89 (s, 3H), 1.43 (d, *J* = 0.9 Hz, 9H).

V.3.9. Tert-butyl(methyl)(2-oxoethyl)carbamate

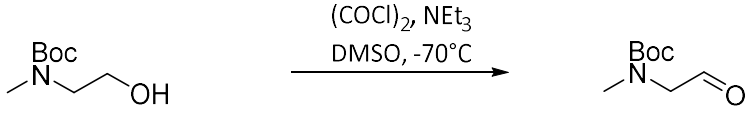

11 **12**

Substances	equivalent	n [mmol]	M [g/mol]	m /V
11	1	12	175.12	2.1 g
$(COCl)_2$	1.5	18	126.93	2.3 g/ 1.54 ml
NEt_3	4.5	54	101.19	5.5g / 7.49 ml
DMSO	3.5	36	78.3	2.8 g/ 2.55 ml

Procedure:

15 ml absolute DCM and $(COCl)_2$ was filled into a flask and cooled to -70°C. 2.55 ml DMSO was slowly added to the mixture. The temperature was set between -60 to -80°C. **11**, which was dissolved in 6 ml absolute DCM, was injected drop by drop through a syringe over 30 min at an average temperature of -75°C. Then, NEt_3 was added. The reaction was monitored by TLC (EE:PE 1:1) until indication of complete conversion. At that point, the solution was quenched by adding a saturated $NaHCO_3$-solution drop-wise. This cloudy solution was extracted with DCM (3x 100 ml) and the combined organic phases were dried over Na_2SO_4, filtered and the solvent was stripped.

Yield: 1.7 g bright green fluid (80.9% of theory)

Analysis:

R_f (PE:EE 1:1): 0.46

H-NMR: ^{1}H NMR (200 MHz, Chloroform-*d*) δ 9.59 (s, 1H), 3.95 (d, *J* = 43.6 Hz, 2H), 2.93 (d, *J* = 13.3 Hz, 3H), 1.54 – 1.33 (m, 9H).

V.3.10. (E)-ethyl-5-((tert-butoxycarbonyl)(methyl)amino)pent-3-enoat

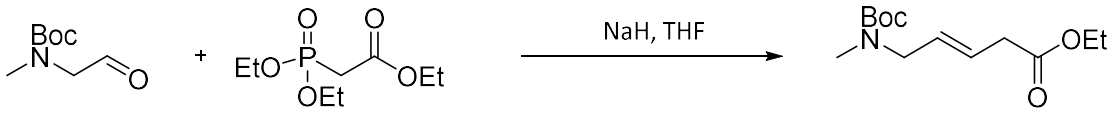

12 **12a** **13**

Substances	equivalent	n [mmol]	M [g/mol]	m /V
12	1	5.76	173.11	1 g
12a	2.3	13.28	224.19	3 g / 2.64 ml
NaH	2	11.56	23.49	0.460 g

Procedure:

NaH was dissolved in 40 ml THF, stirred and cooled to 0°C. **12a** was added drop-wise, which resulted in a white suspension. This mixture was warmed up to room-temperature before addition of **12**, which was dissolved in 10 ml THF. After 1 h, the mixture turned into a clear yellow solution, which indicated the completion of the reaction. The work-up started with the dilution of the THF-phase which was extracted 3 times with 100 ml EE and dried over Na_2SO_4. The drying-agent was removed by filtration and the filtrate was concentrated in vacuo and purified with silica gel column chromatography (SiO_2 90 g 10→50 30 min 50→100 in 10 min) to give compound 14.

Yield: 0.7 g yellow oil (50 % of theory)

Analysis:

R_f (PE:EE 1:1): 0.74

H-NMR: ^{1}H NMR (400 MHz, Chloroform-*d*) δ 6.83 (dt, *J* = 15.7, 5.1 Hz, 1H), 5.86 (t, *J* = 1.8 Hz, 1H), 4.18 (d, *J* = 7.2 Hz, 2H), 4.03 – 3.89 (m, 2H), 2.83 (s, 4H), 1.44 (s, 12H), 1.28 (t, *J* = 7.1 Hz, 3H).

V.3.11. (E)-5-((tert-butoxycarbonyl)(methyl)amino)pent-3-enoic acid

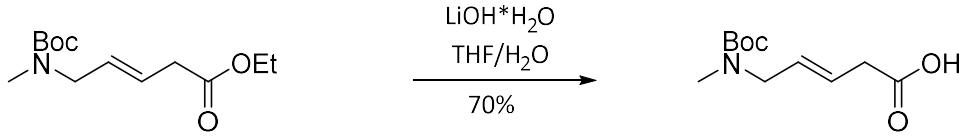

13 **14**

Substances	equivalent	n [mmol]	M [g/mol]	m /V
13	1	7.9	243.15	1.8 g
LiOH*H_2O	5	39.3	41.96	1.65 g

Procedure:

13 was dissolved in 45 ml THF and bubbled wit Argon. LiOH was dissolved in 30 ml THF and injected to the solution drop by drop. After a reaction time of 12 h, TLC showed full conversion of the educt. THF was evaporated and the resulting yellow aqueous solution was acidified with 1 N HCl to pH 3 and extracted with EE (4x 100 ml). The combined organic phase was dried over Na_2SO_4, the work-up was concluded by a chromatography step (SiO2 8g 0→15% in 30 min 15→15% for 30 min DCM:Methanol)

Yield: 1.4 g bright brown-yellow solid(60% of theory)

Analysis:

R_f (DCM:Methanol 10:1): 0.9

H-NMR: ^{1}H NMR (400 MHz, Chloroform-*d*) δ 6.95 (dt, *J* = 15.7, 5.0 Hz, 1H), 5.85 (d, *J* = 15.7 Hz, 1H), 4.00 (d, *J* = 15.1 Hz, 2H), 2.86 (s, 3H), 1.45 (s, 8H).

V.3.12. (R,E)-tert-butyl (4-(3-(4-amino-3-(4-phenoxyphenyl)-1H-pyrazolo[3,4-d]pyrimidin-1-yl)piperidin-1-yl)-4-oxobut-2-en-1-yl)(methyl)carbamate

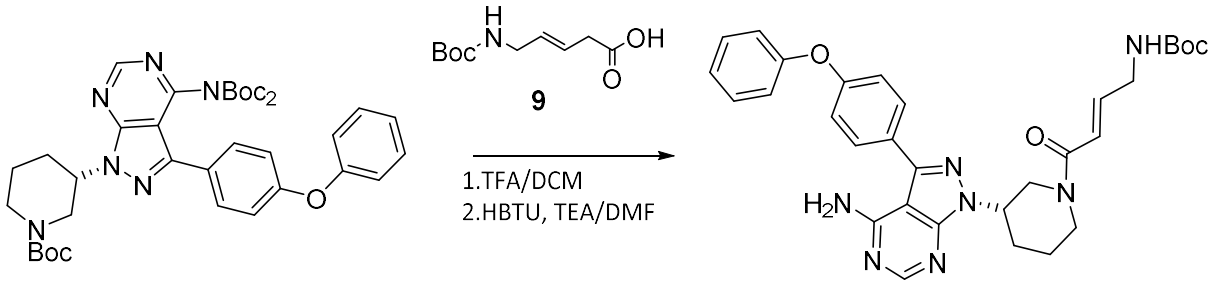

6 15

Substances	equivalent	n [mmol]	M [g/mol]	m /V
6	1	0.44	686.34	0.3 g
TFA			114.02	1.5ml
DCM				4.5 ml
9	1.15	0,51	201.10	0.1 g
HBTU	1.5	0,66	379.24	0.25 g
TEA				0.3 ml
DMF				5 ml

Procedure:

6 was dissolved in 4.5 ml absolute DCM and filled into a vial. After the mixture was bubbled with argon for 15 min, 1.5 ml TFA was added. Once LC-MS showed full removal of protective group, the solution was concentrated in vacuo and azeotrope distillation with a mixture of DCM:ACN (1:1) was carried out five times.

9 and HBTU were dissolved in 4 ml DMF and TEA, which is dissolved in 0.6 ml DMF, and added drop-wise to this solution. Therefore, the color of the solution changed from intense blue to a dark-yellow-brown. After 1 h the crude-product from step one, which is dissolved in 0.4 ml DMF, was added to the solution. After 2 h, LC-MS indicated full conversion and the solution was directly loaded onto a C18 reverse phase column (10→50% in 5 min 50→60% in 20 min 60→90 in 5 min H2O(0.1%FA):ACN(0.1%FA))

Yield: 0.12 g bright brown solid (48% of theory)

Analysis:

H-NMR: ^{1}H NMR (400 MHz, Chloroform-*d*) δ 8.19 (d, *J* = 47.0 Hz, 1H), 7.66 – 7.47 (m, 1H), 7.44 – 7.23 (m, 1H), 7.20 – 6.95 (m, 3H), 6.68 (s, 1H), 6.31 (t, *J* = 18.0 Hz, 1H), 6.03 (s, 1H), 4.73 (d, *J* = 41.5 Hz, 1H), 3.85 – 3.74 (m, 1H), 2.15 (d, *J* = 37.4 Hz, 1H), 1.94 (s, 1H), 1.46 – 1.08 (m, 5H).

V.3.13. (R,E)-tert-butyl (4-(3-(4-amino-3-(4-phenoxyphenyl)-1H-pyrazolo[3,4-d]pyrimidin-1-yl)piperidin-1-yl)-4-oxobut-2-en-1-yl)carbamate

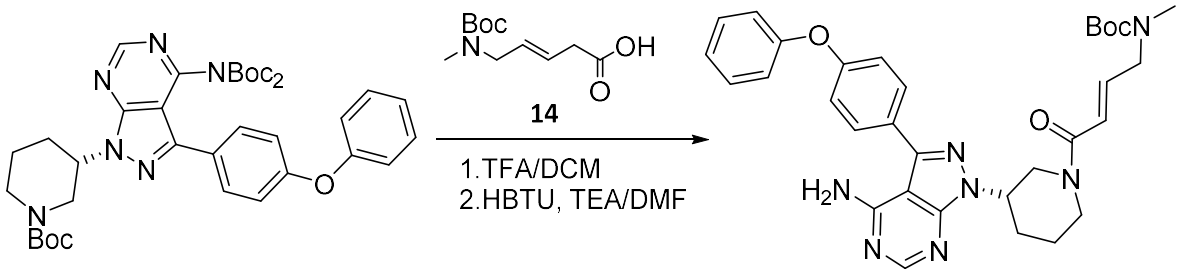

6 **16**

Substances	equivalent	n [mmol]	M [g/mol]	m /V
6	1	0.73	686.34	0.5 g
TFA			114.02	3.3 ml
DCM				6.6 ml
14	1.15	0.84	201.10	0.18 g
HBTU	1.5	1.1	379.24	0.42 g
TEA				0.5 ml
DMF				7.3 ml

Procedure:

6 was dissolved in 6.6 ml absolute DCM and filled into a Vial. After the mixture was bubbled for 20 min 3.3 ml TFA was added. After LC-MS showed full removal of protective group, the solution was concentrated in vacuo and azeotrope distilled with a mixture of DCM:ACN (1:1) five times.

14 and HBTU were dissolved in 6 ml DMF and TEA, which was dissolved in 0.8 ml DMF, was added drop-wise to this solution. Therefore, the solution color changed from intense blue to dark-yellow-brown. After 1 h, the crude-product from step one, dissolved in 0.5 ml DMF, was added to the solution. After 2 h, LC-MS indicated full conversion and the solution was directly loaded onto a C18 reverse phase column (10→50% in 5 min 50→60% in 25 min 60→90 in 5 min H_2O(0.1%FA):ACN(0.1%FA))

Yield: 0.18 g bright brown solid (42.3% of theory)

Analysis:

H-NMR: ^{1}H NMR (400 MHz, Chloroform-*d*) δ 8.34 (d, *J* = 10.0 Hz, 1H), 7.62 (d, *J* = 8.5 Hz, 2H), 7.48 – 7.34 (m, 2H), 7.31 – 7.01 (m, 5H), 6.74 (s, 1H), 6.29 (s, 2H), 4.87 (s, 1H), 4.60 (s, 1H), 4.16 (d, *J* = 13.1 Hz, 0,5H), 3.95 (d, *J* = 22.5 Hz, 2H), 3.73 (t, *J* = 12.0 Hz, 0,5H), 3.36 (t, *J* = 11.7 Hz, 0,5H), 3.18 (t, *J* = 12.2 Hz, 0,5H), 3.01 – 2.61 (m, 4H), 2.44 – 2.16 (m, 2H), 1.98 (d, *J* = 10.4 Hz, 1H), 1.71 (d, *J* = 12.7 Hz, 1H), 1.46 (s, 9H)

V.3.14. 5-CyanoCyclooctene

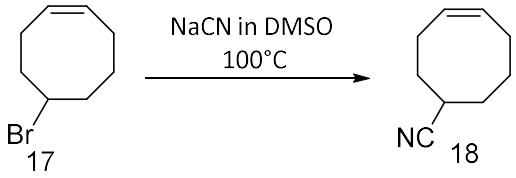

Substances	equivalent	n [mmol]	M [g/mol]	m /V
17	1	476	189.10	90 g
NaCN	1.2	571	49.01	28 g
DMSO				270

Procedure:

NaCN was dissolved in DMSO (200 ml), and **17** in 70 ml DMSO was added drop-wise to the reaction mixture at 100°C, which created a brown solution. After 15 min, the solution was cooled to r.t. and was added to 1500 ml of a water-ice mixture. This aqueous solution was mixed with DE and extracted 4 times. The organic phase was washed with brine and dried over $NaSO_4$. After the solvent was removed, this crude was used for further reactions.

Yield: 39,8 g (62% of theory)

Analysis:

R_f(PE:EA = 5:1) = 0.6

H-NMR: ^{1}H NMR (400 MHz, Chloroform-*d*): δ 5.79 – 5.51 (m, 2H), 2.85 – 2.72 (m, 1H), 2.47 – 1.71 (m, 7H), 1.62 – 1.30 (m, 2H).

V.3.15. 5-Iodo-1-methyl-7-oxabicyclo[4.2.2]decan-8-one

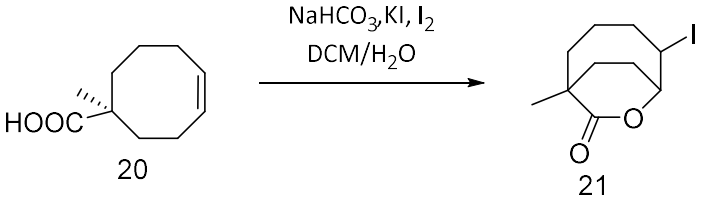

20 21

Substances	equivalent	n [mmol]	M [g/mol]	m /V
20	1	15.5	168.24	2.6 g
$NaHCO_3$	3.3	51.15	84	4.29 g
KI	3	46.5	166.8	7.76 g
Iodine	2	31	253.81	7.87 g
DCM				22 ml
H_2O				22 ml

Procedure:

20 was dissolved in DCM (20 ml) and added to a solution of $NaHCO_3$ in water (20 ml), which resulted in a two phase-system. This mixture was cooled to 0°C. Afterwards, a mixture of KI and I_2 was added over one hour in 5 portions over a time of 45 min. The result was a brown mixture, which stirred for 4 h. Then, it was quenched with $NaHSO_3$ until the brown color was not visible anymore. The aqueous phase was extracted with DCM 5 times with 20 ml solvent each. These organic layers were combined and dried over Na_2SO_4 and the solvent was removed under low pressure to give the product **21**

Yield: 4.2g yellow solid (92 % of theory)

Analysis:

R_f(PE:EA = 6:1) = 0.57

H-NMR: ^{1}H-NMR (400 MHz, $CDCl_3$): δ = 5.00 – 4.91 (m, 1H), 4.58 – 4.42 (m,1H), 2.43 – 1.45 (m, 10H), 1.25 (s, 3H) ppm.

V.3.16. (Z)-1-Methyl-7-oxabicyclo[4.2.2]dec-4-en-8-one

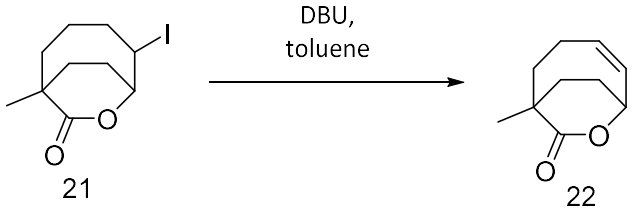

Substances	equivalent	n [mmol]	M [g/mol]	m /V
21	1	14,4	294.13	4.2 g
DBU	1.7	24.5	152.24	3.7 g
Toluene				17 ml

Procedure:

Component **21** was mixed with 17 ml toluene and DBU was added. This reaction-mixture stood at r.t. for 18 hours and afterwards was heated under reflux for 1 ½ h. After cooling to r.t., the organic phase was washed 5 times with 20 ml water. These aqueous layers were extracted with a small amount of toluene (20 ml) one time and combined to dry it over Na_2SO_4. After the solvent was removed, final purification was done with the Kugel distillation (0.6 mbar 120-160°C) to get product **22.**

Yield: 1.8 g yellow oil (75 % of theory)

Analysis:

H-NMR: ^{1}H NMR (400 MHz, Chloroform-*d*) δ 5.73 – 5.53 (m, 1H), 5.38 – 5.3 (m, 1H), 4.99 (s, 1H), 2.51 – 2.33 (m, 1H), 2.29 – 2.22 (m, 2H), 2.01– 1.62 (m, 5H), 1.26 (s, 3H) ppm.

V.3.17. Methyl (Z)-6-hydroxy-1-methylcyclooct-4-ene-1-carboxylate

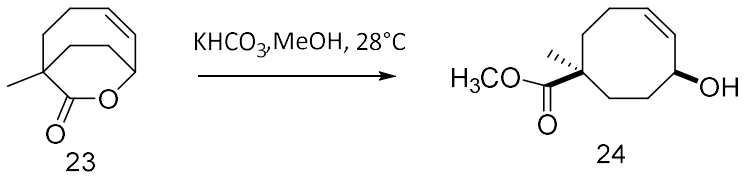

Substances	equivalent	n [mmol]	M [g/mol]	m /V
23	1	10.7	166.22	1.8 g
$KHCO_3$	4	42.8	100.12	4.3 g
MeOH				12 ml

Procedure:

A mixture of $KHCO_3$ and compound **23** was combined with MeOH (12 ml) and stirred for 3 days at 28 °C. The resulting suspension was filtrated and washed with MeOH. Finally, the solvent was removed with a rotary evaporator. The crude product was take up by a mixture of DCM with water. The aqueous phase was washed with more DCM and the combined organic layers were died over Na_2SO_4. After the solvent was removed, product **24** could be isolated.

Yield: 1.1 g yellow oil (52 % of theory)

Analysis:

R_f(PE:EA = 3:2) = 0.28

H-NMR: ^{1}H NMR (400 MHz, Chloroform-*d*) δ 5.73 – 5.53 (m, 1H), 5.38 – 5.21 (m, 1H), 4.85 – 4.67 (m, 1H), 3.62 (s, 3H), 2.40 – 1.50 (m, 9H), 1.32 (s, 3H).

V.3.18. Methyl (E)-6-hydroxy-1-methylcyclooct-4-ene-1-carboxylate

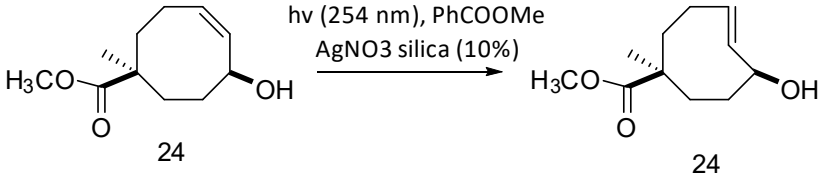

Substances	equivalent	n [mmol]	M [g/mol]	m /V
24			198,26	1 g
Methyl benzoate			136,15	1.4 g/1.3 ml
$AgNO_3$ silica (10%) (SIGMA)				15 g
Et_2O:heptane (1:1)				200 ml

Equipment:

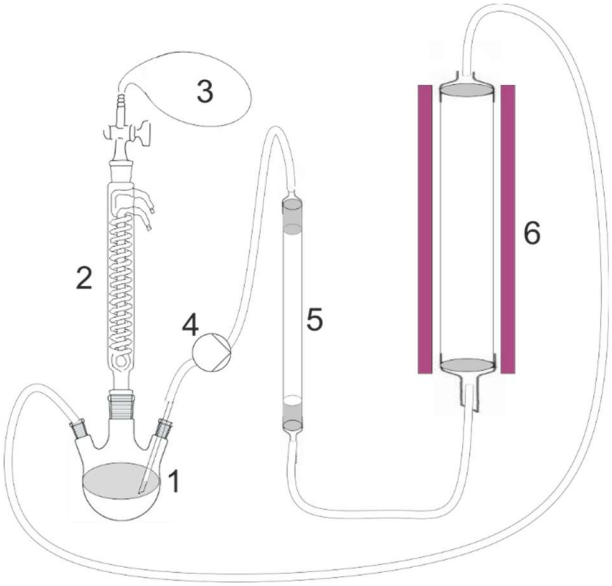

1…three-neck-flask (500 ml)
2…reflux condenser
3…argon balloon
4…pump
5…column (15 g AgNO3 impregnated silica (10%) between two layers of silicagel)
6… quartz glass tube with one 55 W low-pressure mercury lamps emitting a dominant wavelength of 254 nm

Procedure:

As a first step, the isomerization system was washed and conditioned with heptane/Et_2O mixture. Afterwards, 200 ml of the same mixture was filled into the flask and pumped into the whole system. Then the methylbenzoate was dissolved in 10 ml heptane/Et_2O and added to the circulating solvent. After 30 min of homogenization, the educt was injected to the reaction mixture. Equilibration was obtained by circulating the solution for 20 min before it was irradiated for 12 h.

As next step the column was washed with Et_2O and dried via air-flow (to remove methyl benzoatee and traces of the *cis*-Cyclooctene). Trough methanolic ammonia solution the TCO was transferred from the column into solution. The crude solution was concentrated via rotary evaporation and then purified by vacuum filtration over silica gel. The solvent was again removed in vacuum to get a brightly yellow fluid as mixture of two diastereomers. This mixture of two diastereomers was used directly in the next reaction.

Yield: 0.7 g yellow oil (70 % of theory)

equatorial (with regard to the hydroxyl functionality) in a ratio of 1:1.8 (=axial:equatorial).

Analysis:

axial isomer:

R_f(PE:EA = 2:1) = 0.45

H-NMR: ^{1}H NMR (400 MHz, Chloroform-*d*) δ 6.14 – 5.96 (m, 1H), 5.62 (dd, *J* = 16.6, 2.6 Hz, 1H), 3.64 (d, *J* = 13.4 Hz, 4H), 2.40 – 1.64 (m, 8H), 1.31 – 1.17 (m, 1H), 1.10 (s, 3H).

equatorial isomer:

R_f(PE:EA = 2:1) = 0.36

H-NMR: ^{1}H NMR (400 MHz, Chloroform-*d*) δ 5.77 (ddd, *J* = 15.9, 11.6, 4.0 Hz, 1H), 5.34 (dd, *J* = 16.2, 9.4 Hz, 1H), 4.26 – 4.10 (m, 1H), 3.71 (s, 3H), 2.78 – 2.57 (m, 1H), 2.30 – 2.16 (m, 2H), 2.13 – 2.02 (m, 3H), 1.97 – 1.84 (m, 1H), 1.81 – 1.72 (m, 1H), 1.50 (ddd, *J* = 14.2, 12.5, 4.8 Hz, 2H), 1.18 (s, *J* = 2.7 Hz, 3H).

V.3.19. rel-(1R,4E,6R,pS)-6-Hydroxy-1-methylcyclooct-4-ene-1-carboxylic acid

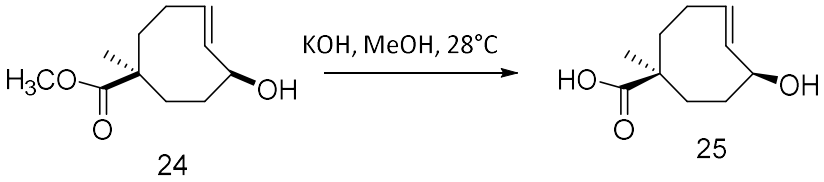

24 25

Substances	equivalent	n [mmol]	M [g/mol]	m /V
24	1		87,8	0.7 g
KOH	11,5		100,9	2.3 g
Citric acid				6.6 g
MeOH: H_2O				16 ml: 7.4 ml

Procedure:

The mixture of the two diastereomers were dissolved in absolute methanol and bubbled with argon. The next step was to add KOH drop-wise while the reaction mixture was cooled. After 12 h, TLC showed full conversion and the solution was diluted with 20 ml H_2O and extracted 3 times with 80 ml MTBE. The aqueous phase was again diluted with water and acidified with 6.6 g citric acid. The same washing step was repeated, and the final solution concentrated in vacuo to attain the final diastereomer-clear product.

Yield: 0,45 g yellow oil (60% of theory)

Analysis:

H-NMR: ^{1}H NMR (400 MHz, Chloroform-*d*) δ 6.14 – 5.96 (m, 1H), 5.64 (dd, *J* = 16.5, 2.7 Hz, 1H), 4.52(b.s., 1H), 2.39 – 1.60 (m, 8H), 1.12 (s, 3H).

V.3.20. rel-(1R,4E,6R,pS)-2,5-Dioxopyrrolidin-1-yl-6-((((2,5-di-oxopyrrolidin-1- yl)oxy)carbonyl)oxy)-1-methylcyclooct- 4-ene-1-carboxylate

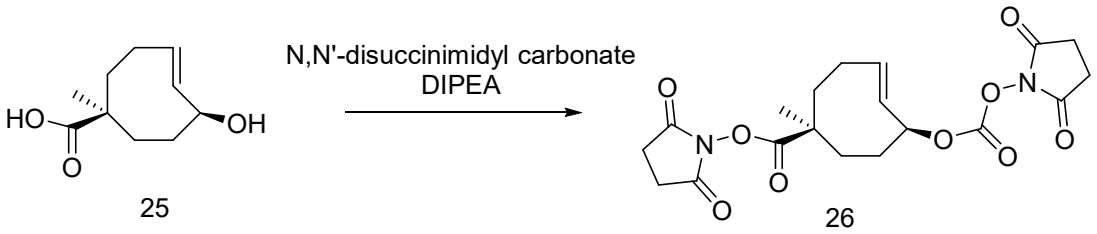

25 26

Substances	equivalent	n [mmol]	M [g/mol]	m /V
25	1	1.09	184.24	0.2 g
N,N'-Disuccinimidyl carbonate	4.3	4.67	256.17	1.2g
Diisopropylethylamine	7.4	8.07	129.24	1.04 g/ 1.38 ml
DMAP	0.5	0.55	122.17	0.065 g

Procedure:

Compound **25**, N,N'-Disuccinimidyl carbonate and DMAP were dissolved in 7 ml absolute ACN which lead to a yellow suspension. DIPEA was added to the suspension, therefore it changed from a yellow suspension to an orange one. After 4 days, LC-MS indicated the complete conversion of the reaction. Thus, the reaction-mixture was filtrated and washed with ACN. The filtrate was concentrated in vacuo and taken up in 10 ml DCM to wash it 3 times with 20 ml H_2O and finally the solvent was removed again.

Yield: 0,12 g white solid (25% of theory)

Analysis:

H-NMR: 1H NMR (400 MHz, Chloroform-d) δ 6.07 (ddd, J = 16.7, 10.6, 3.5 Hz, 1H), 5.62 (dd, J = 16.7, 2.6 Hz, 1H), 5.33 – 5.24 (m, 1H), 2.84 (s, 8H), 2.50 – 2.23 (m, 4H), 2.20 – 1.93 (m, 4H), 1.27 (s, 3H).

V.3.21. d-TCO-PEG

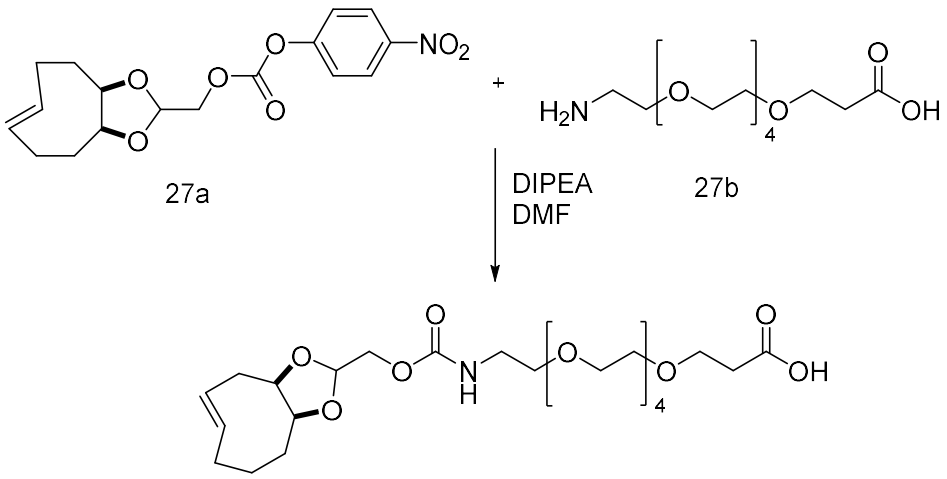

27

Substances	equivalent	n [mmol]	M [g/mol]	m /V
27a	1	0.0714	349.12	25 mg
27b	1,2	0.0857	353.41	30 mg
DIPEA				0.2 ml
DMF				1 ml

Procedure:

27a was filled into a Vial purged with Argon and 2 ml DMF and 2 drops of DIPEA were added. The conversion of the reaction was monitored via LC-MS and after full conversion the mixture was directly loaded onto a C18 column for final purification. The ultimate product was directed used without further characterization for the subsequent reaction.

Yield: crude 30 mg

V.3.22. d-TCO-PEG-Ibrutinib

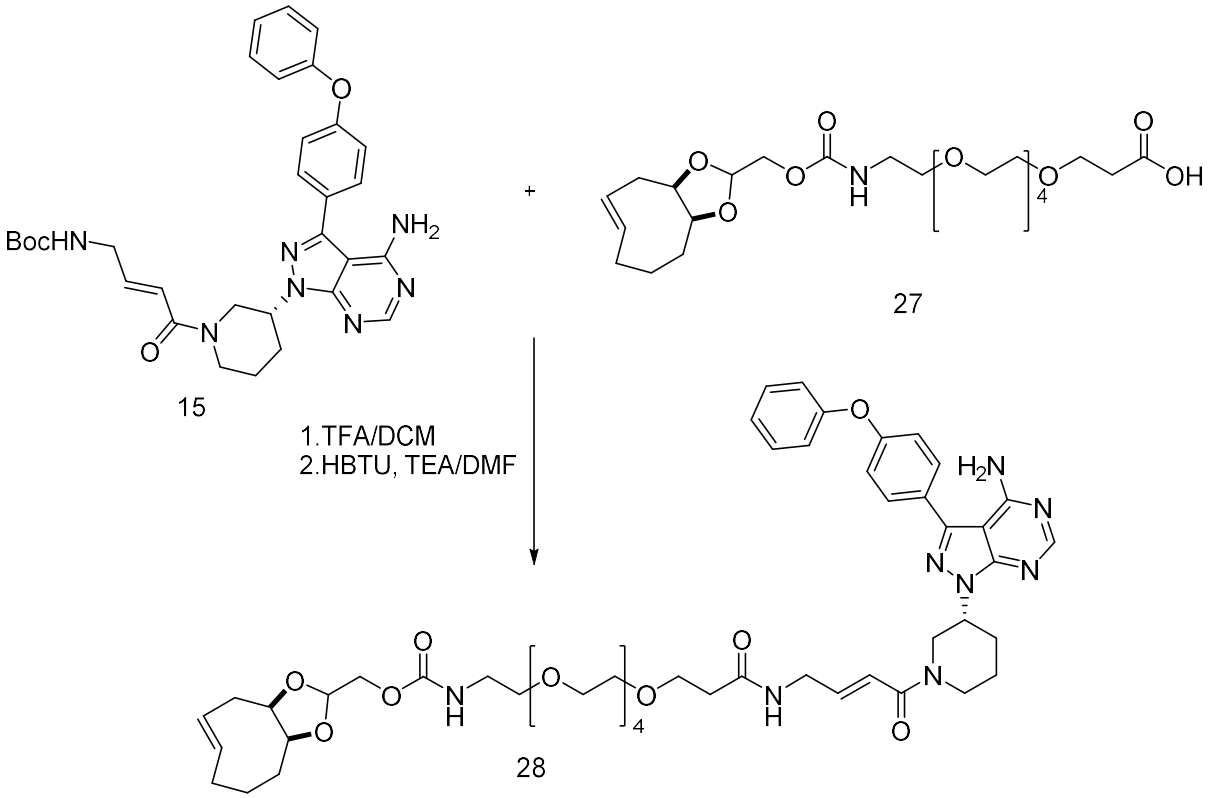

Substances	equivalent	n [mmol]	M [g/mol]	m /V
15	1	0.0532	568.64	25 mg
DCM				600 µl
TFA				150 µl
27	1.15	0.0612	505.41	30mg
HBTU	1.5	0.0798	379.24	30 mg
TEA	5	0.266	101.19	26 mg / 36 µl
DMF				750 µl

Procedure:

Solution 1: **15** was dissolved in DCM and TFA was added drop-wise to the reaction. The deprotection reaction was monitored via LC-MS until complete conversion. The mixture was concentrated in high vacuum and then co-evaporated wit DCM/ACN to remove TFA. The crude product was dissolved in 0.5 ml DMF and 2 drops of DIPEA were added.

Solution 2: **27** and HBTU were dissolved in DMF and flushed with Argon and TEA was added. Afterwards, 4 drops of DIPEA were added to the mixture, changing the color from colorless to yellow-brown.

After 30 min, Solution 1 was added to Solution 2 drop by drop and after 2 hours this mixture was directly loaded onto an C18 column to get the final product.

Yield: 15 mg white solid

Analysis:

H-NMR: ^{1}H NMR (600 MHz, DMSO-d_6) δ 8.25 (d, *J* = 10.7 Hz, 1H), 7.65 (d, *J* = 8.5 Hz, 2H), 7.43 (dd, *J* = 8.6, 7.3 Hz, 2H), 7.21 – 7.06 (m, 5H), 6.97 – 6.88 (m, 1H), 6.62 – 6.47 (m, 1H), 5.66 – 5.37 (m, 2H), 4.73 – 4.60 (m, 1H), 4.55 – 4.46 (m, 1H), 4.26 – 3.73 (m, 3H), 3.61 (d, *J* = 11.1 Hz, 3H), 3.51 – 3.43 (m, 37H), 3.12 – 3.01 (m, 3H), 2.26 (td, *J* = 6.3, 3.0 Hz, 5H), 2.09 (dq, *J* = 13.8, 6.0 Hz, 2H), 1.94 – 1.79 (m, 5H), 1.70 – 1.43 (m, 6H).

C-NMR: 13C NMR (151 MHz, DMSO-d6) δ 169.57, 169.00, 158.22, 157.13, 156.34, 155.83, 143.34, 141.91, 134.95, 132.55, 130.18, 123.83, 120.34, 119.87 – 118.00 (m), 79.09, 74.45, 69.79, 67.14, 47.60, 44.45, 33.79, 32.19, 30.62, 25.17, 24.59, 21.95, 21.03, 20.23, 16.52, 14.98.

V.3.23. standard-TCO-PEG

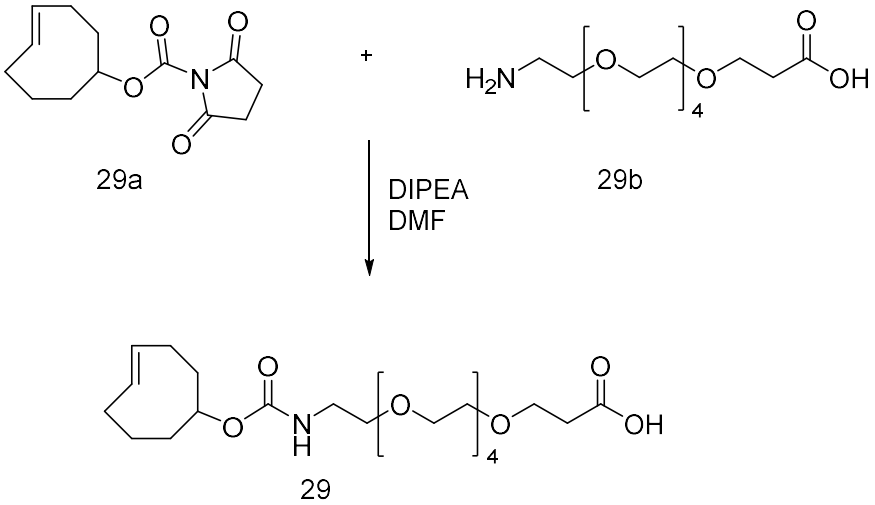

Substances	equivalent	n [mmol]	M [g/mol]	m /V
29a	1	0.075	267.28	20 mg
29b	1,2	0.089	353.41	32 mg
DIPEA				0.2 ml
DMF				1 ml

Procedure:

29a in DMF was combined with **29b** and DIPEA was added to the solution. This mixture was stirred for 2 h until LC-MS analysis indicated the complete consumption of the starting material. Finally, the reaction mixture was purified by preparative reverse phase chromatography. The Product was directly used for the following reaction without further characterization.

Yield: 30 mg crude (60% of theory)

V.3.24. standard-TCO-PEG-Ibrutinib

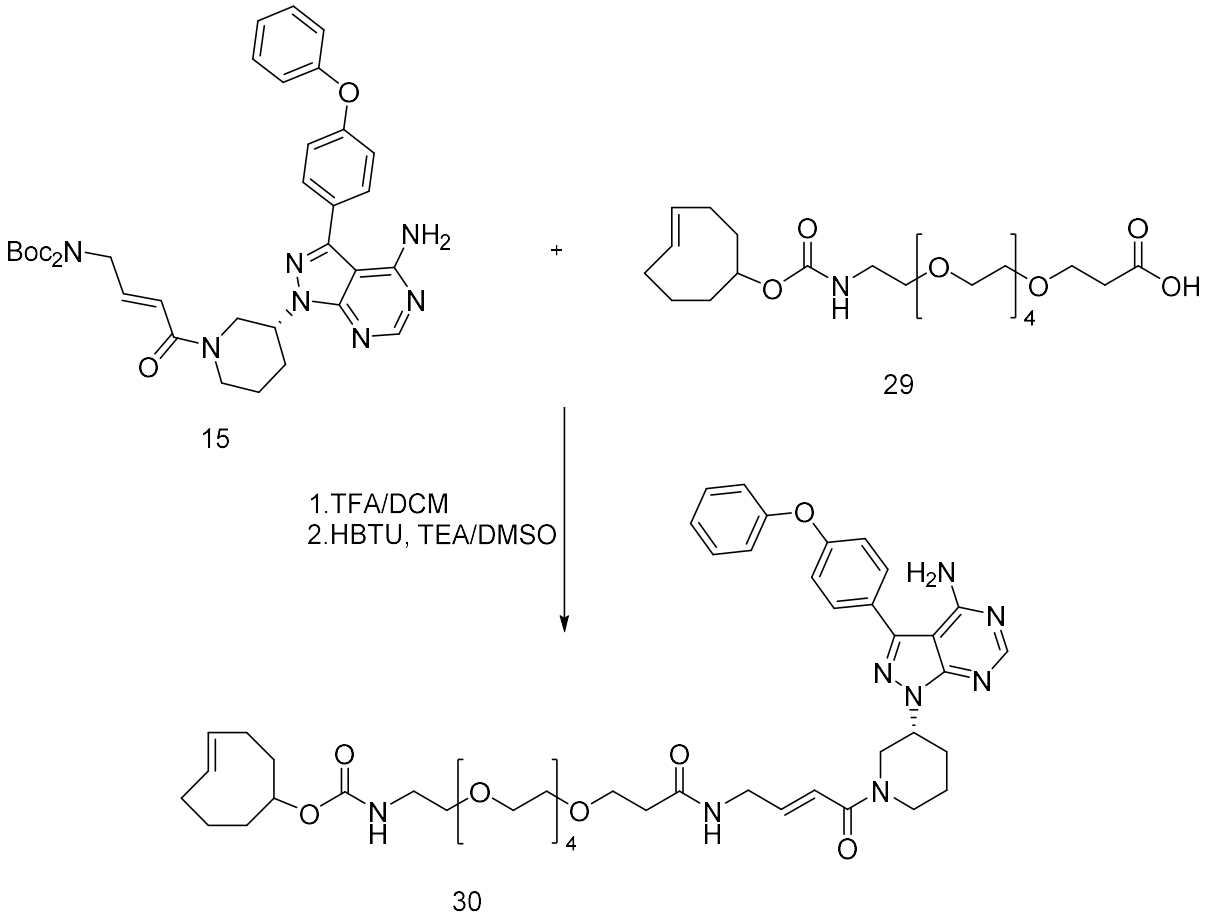

Substances	equivalent	n [mmol]	M [g/mol]	m /V
15	1	0.044	568.64	25 mg
DCM				600 µl
TFA				150 µl
27	1,15	0.0505	353.41	18 mg
HBTU	1,5	0.0758	379.24	30 mg
TEA	5	0.22	101.19	22 mg / 32 µl
DMF				750 µl

Procedure:

Solution 1: TFA and DCM was filled into a vial which contained the ibrutinib-derivate. After the deprotecting-reaction was completed, which was indicated by LC-MS, TFA and DCM were removed in vacuo via azeotrope-distillation with DCM/ACN 5 times. The crude product was dissolved in DMSO with 2 drops of TEA.

Solution 2: A vial was charged with **29**, HBTU, DMSO and TEA and stirred overnight. Afterwards, Solution 1 was added to Solution 2 drop-wise. The conversion of the reaction was monitored via LC-MS and the product was finally purified via reverse phase chromatography.

Yield: 15 mg white solid (60% of theory)

Analysis:

H-NMR: ^{1}H NMR (600 MHz, DMSO-d_6) δ 8.28 – 8.21 (m, 1H), 8.14 (t, *J* = 5.8 Hz, 1H), 7.65 (d, *J* = 8.6 Hz, 2H), 7.49 – 7.34 (m, 2H), 7.21 – 7.07 (m, 5H), 6.64 – 6.46 (m, 1H), 5.54 (qdd, *J* = 17.0, 9.1, 5.1 Hz, 1H), 4.73 – 4.61 (m, 1H), 4.18 – 3.73 (m, 6H), 3.54 – 3.43 (m, 20H), 3.10 (dd, *J* = 5.8, 3.4 Hz, 2H), 2.37 (d, *J* = 4.0 Hz, 1H), 2.26 (dd, *J* = 13.0, 6.6 Hz, 2H), 2.10 (tdt, *J* = 18.7, 13.3, 6.4 Hz, 2H), 1.98 – 1.44 (m, 5H).

^{13}C NMR (151 MHz, DMSO-d_6) δ 170.64, 164.88, 158.64, 156.74, 156.20, 143.76, 142.15, 136.52, 130.60, 128.35, 124.26, 120.74, 119.42, 99.00, 80.24, 70.21, 69.47, 67.26, 64.63, 52.50, 49.58, 46.16, 36.52, 30.11, 25.55.

V.3.25. Methyl-Ibrutinib-Sir-COOH

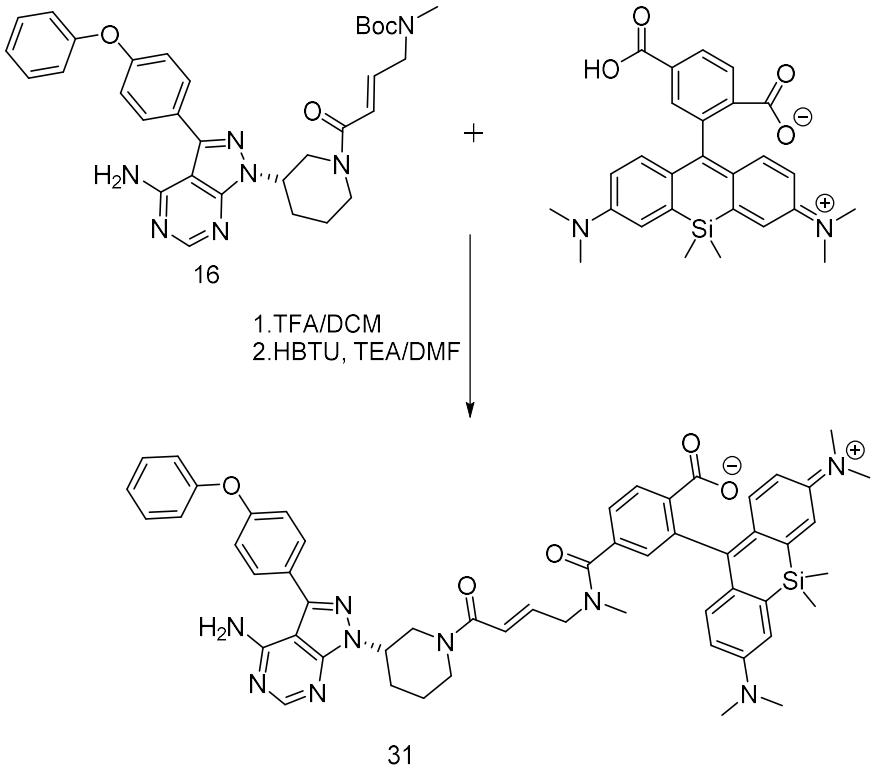

Substances	equivalent	n [mmol]	M [g/mol]	m /V
15	1	0.017	583.29	10 mg
DCM				200 µl
TFA				50 µl
SIR-dye	1,15	0.020	472.18	9.5 mg
HBTU	1,5	0.026	379.24	10 mg
TEA	5	0.085	101.19	8.6 mg / 12 µl
DMF				250 µl

Procedure:

Solution 1: A vial was charged with DCM and the ibrutinib-derivate and TFA was added. The deprotecting-reaction was monitored via LC-MS. After full conversion, TFA and DCM was removed via azeotrope-distillation with DCM/ACN 5 times. The crude product was dissolved in DMF with one drop of TEA.

Solution 2: To a solution of SIR-COOH, HBTU and DMF, TEA was added drop-wise. As a result, the color changed from intense blue to dark brown.

After 2 h, solution 1 was added to the solution 2. The full conversion of the reaction was indicated by LC-MS and the product was directly loaded onto a C18 Column.

Yield: 4 mg blue solid (60% of theory)

Analysis:

H-NMR: 1H NMR (400 MHz, DMSO-d6) δ 9.08-8.92 (m, 1H), 8.35 -7.96(m, 4H), 7.73 (d, *J* = 13.3 Hz, 1H), 7.69-7.40 (m, 4H), 7.30-7.05 (m, 5H), 7.05 (s, 2H), 6.66-6.42 (m, 6H), 4.80-4.63 (m, 1H), 4.28-3.93 (m, 3H), 3.72-3.5 (s, 3H) 3.25-2.99 (m, 2H), 2.93 (s, 12H), 2.38-2.01 (m, 2H), 1.93-1.50 (m, 2H), 0.7 (s, 3H), 0.59(s, 3H).;

V.3.26. Ibrutinib-Sir-COOH

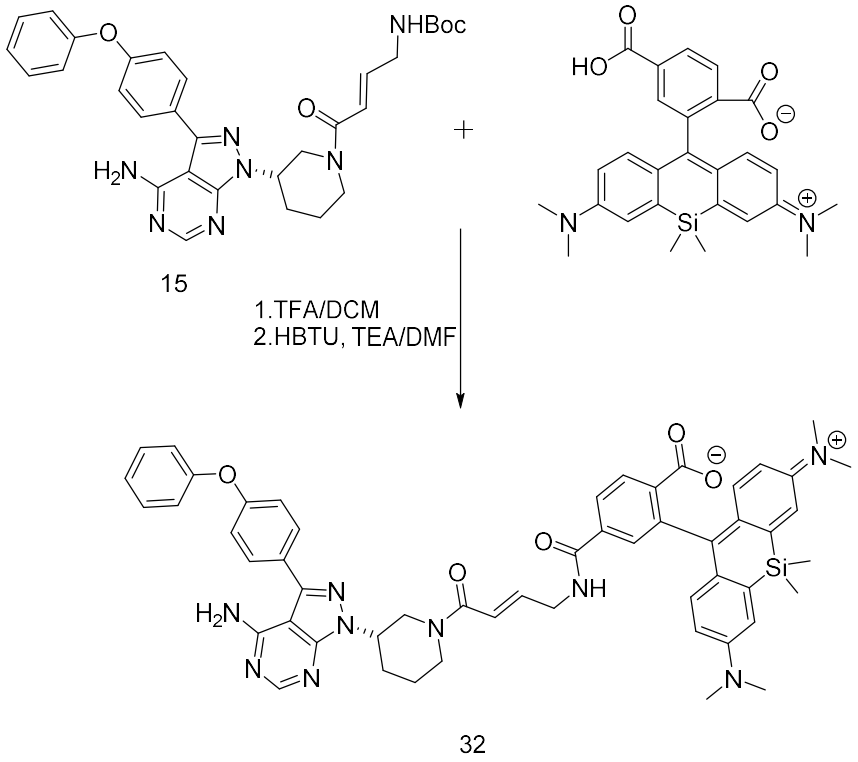

Substances	equivalent	n [mmol]	M [g/mol]	m /V
15	1	0.017	563.64	10 mg
DCM				200 µl
TFA				50 µl
SIR-dye	1,15	0.020	472.18	9.5 mg
HBTU	1,5	0.026	379.24	10 mg
TEA	5	0.085	101.19	8.6 mg / 12 µl
DMF	1	0.017	583.29	10 mg

Procedure:

Solution 1: Compound **15** was dissolved in DCM and TFA was slowly added over a syringe. After the deprotecting-reaction was completed, which was indicated by LC-MS, TFA and DCM were removed in vacuo via azeotrope-distillation with DCM/ACN 5 times. The residue was dissolved in DMF to reach a concentration of 0,1 M in the end solution of compound **15.**

Solution 2: SIR-COOH, HBTU were added to DMF. After TEA was added drop-wise, the color of the solution changed from dark blue to bright brown.

After 2h of reaction time for solution 2, solution 1 was added drop-wise. The full conversion of the reaction was indicated by LC-MS and the product was directly loaded onto a C18 Column.

Yield: 5 mg blue solid

Analysis:

H-NMR: 1H NMR (400 MHz, DMSO-d6) δ 9.05-8.88 (m, 1H), 8.40-7.95 (m, 4H), 7.73-7.38 (m, 4H), 7.24-7.08 (m, 5H), 7.03 (s, 2H), 6.71-6.52 (m, 6H), 4.77-4.60 (m, 1H), 4.41 (t, *J* = 14.9 -3.93 (m, 3H), 3.66 (t, *J* = 11.8 Hz, 0.5H), 3.29-3.01 (m, 1.5H), 2.88 (s, 12H), 2.32-2.10 (m, 2H), 1.98-1.83 (m,1H), 1.70-1.49 (m, 1H), 0.68 (s, 3H), 0.55 (s, 3H).;

V.3.27. m-TCO- methyl-Ibrutinib

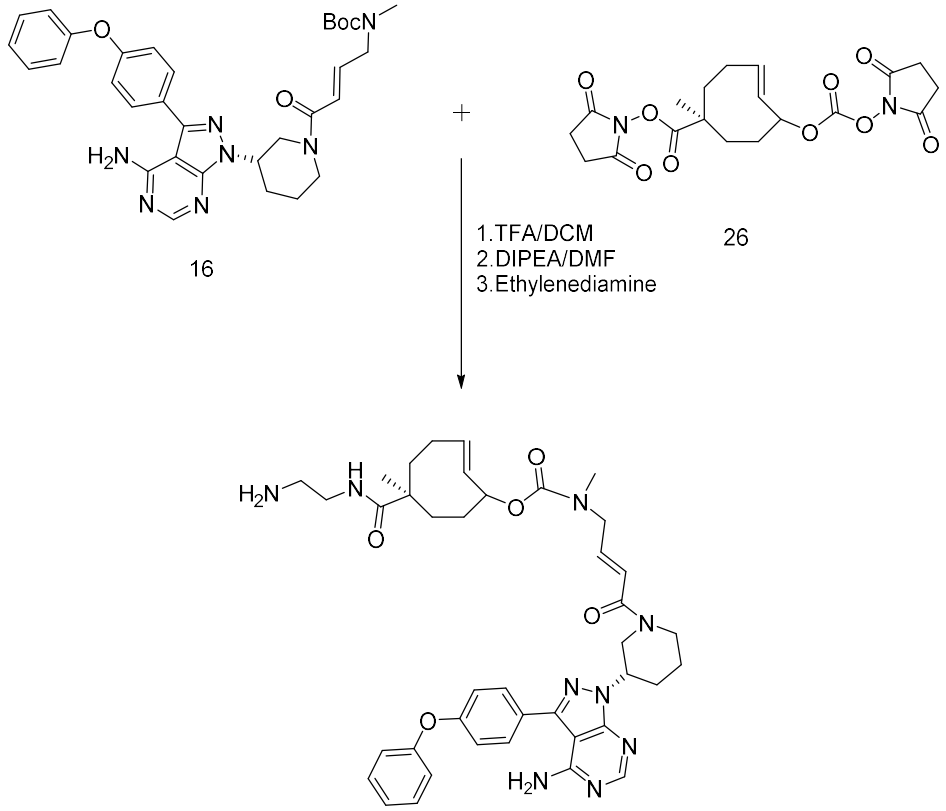

33

Substances	equivalent	n [mmol]	M [g/mol]	m /V
16	1	0.017	583.29	10 mg
DCM				1 ml
TFA				0,333 ml
26	1	0.020	522,13	7.3 mg
DIPEA	3	0.051	129.24	6.6 mg
DMF				0.5 mg
Ethylendiamine	5	0,085	60.10	5.1 mg

Procedure:

To a solution of **16** and DCM, TFA was added. After 30 min, the deprotecting-reaction was completed and the TFA and DCM could be removed via azeotrope-distillation with DCM/ACN 5 times. Afterwards, the crude product was dissolved in 0.5 ml DMF with 3 drops of DIPEA and m-TCO-NHS-ester, which was dissolved in DMF with 1 drop of DIPEA, was added to the mixture. After full conversion to this crude solution, ethylenediamine was added and this mixture was stirred overnight. The solution was directly loaded onto a C18 column to get **33**, which was directly used for the next reaction without further characterization.

Yield: 12 g white solid (96% of theory)

V.3.28. Sir-COOH -m-TCO-methyl-Ibrutinib

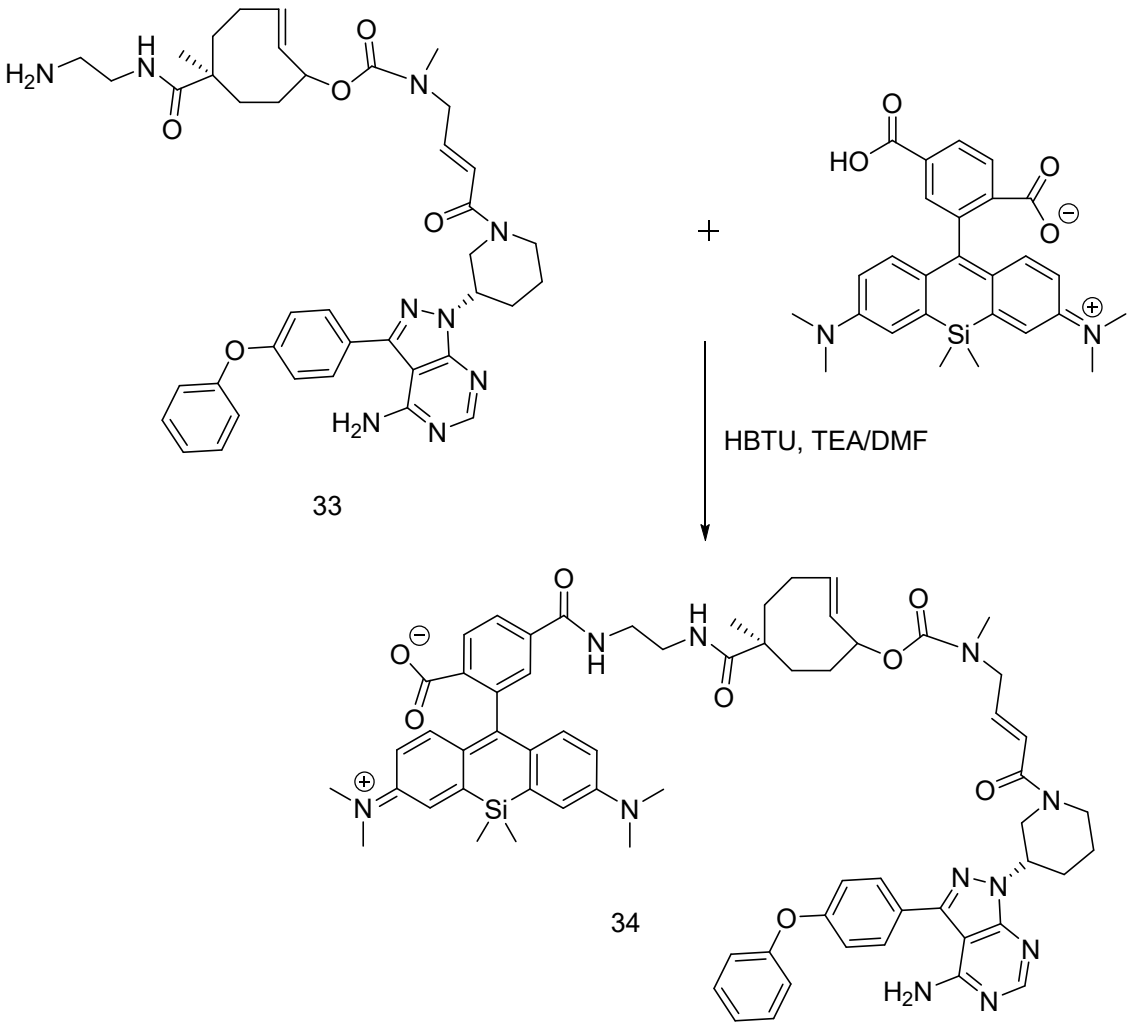

33

34

Substances	equivalent	n [mmol]	M [g/mol]	m /V
33	1	0.017	735.39	12 mg
SIR-dye	1	0.017	472.18	8 mg
HBTU	1,5	0.026	379.24	10 mg
DIPEA	3	0.051	129.24	7.3 mg
DMF				1 ml

Procedure:

Solution 1: A vial was charged with DCM and the ibrutinib-derivate and TFA was added. The deprotecting-reaction was monitored via LC-MS. After full conversion, TFA and DCM was removed via azeotrope-distillation with DCM/ACN 5 times. The crude product was dissolved in DMF with one drop of TEA.

Solution 2: To a solution of SIR-COOH, HBTU and DMF, TEA was added drop-wise. As a result, the color changed from intense blue to dark brown.

After 2 h, solution 1 was added to solution 2. The full conversion of the reaction was indicated by LC-MS and the product was directly loaded onto a C18 Column.

Yield: 4 mg blue solid

Analysis:

H-NMR: ^{1}H NMR (600 MHz, DMSO-d_6 δ 8.69 (s, 1H), 8.34 (s, 1H), 8.24 (s, 1H), 8.01 (s, 3H), 7.62 (d, *J* = 16.1 Hz, 2H), 7.42 (t, *J* = 7.8 Hz, 2H), 7.21 – 7.09 (m, 5H), 7.00 (d, *J* = 2.6 Hz, 2H), 6.64 – 6.58 (m, 6H), 5.5 (d, *J* = 12.5 Hz, 0.5H), 4.99 (d, *J* = 53.3 Hz, 0.5H), 4.76 – 4.43 (m, 1H), 4.18 – 3.93 (m, 9H), 3.29 – 2.8 (m, 3H), 2.91 (d, *J* = 4.9 Hz, 6H), 2,54 – 1.14 (m, 9H), 0.94 – 0.77 (m, 6H), 0.62 (s, 6H), 0.50 (s, 6H).

Literature

[1] G. T. Hermanson, *Introduction to Bioconjugation*. 2013.

[2] R. Sunasee and R. Narain, "Covalent and Noncovalent Bioconjugation Strategies," *Chem. Bioconjugates Synth. Charact. Biomed. Appl.*, pp. 1–75, 2014.

[3] J. Kalia and R. T. Raines, "Advances in Bioconjugation," *Curr Org Chem*, vol. 29, no. 10, pp. 1883–1889, 2010.

[4] F. M. Veronese and G. Pasut, "PEGylation , successful approach to drug delivery," *Drug Discov. Today*, vol. 10, no. 21, pp. 1451–1458, Nov. 2005.

[5] T. Kurpiers and H. D. Mootz, "Bio-orthogonale Ligation im Fokus," *Angew. Chemie*, vol. 121, no. 10, pp. 1757–1760, Feb. 2009.

[6] J. A. Prescher and C. R. Bertozzi, "Chemistry in living systems," *Nat. Chem. Biol.*, vol. 1, no. 1, pp. 13–21, Jun. 2005.

[7] E. M. Sletten and C. R. Bertozzi, "Bioorthogonal Chemistry: Fishing for Selectivity in a Sea of Functionality," *Angew. Chemie Int. Ed.*, vol. 48, no. 38, pp. 6974–6998, Sep. 2009.

[8] H. Staudinger and J. Meyer, "Über neue organische Phosphorverbindungen III. Phosphinmethylenderivate und Phosphinimine," *Helv. Chim. Acta*, vol. 2, no. 1, pp. 635–646, Jan. 1919.

[9] E. Saxon, J. I. Armstrong, and C. R. Bertozzi, "A " Traceless " Staudinger Ligation for the Chemoselective Synthesis of Amide Bonds."

[10] V. V. Rostovtsev, L. G. Green, V. V. Fokin, and K. B. Sharpless, "A Stepwise Huisgen Cycloaddition Process: Copper(I)-Catalyzed Regioselective 'Ligation' of Azides and Terminal Alkynes," *Angew. Chemie Int. Ed.*, vol. 41, no. 14, pp. 2596–2599, Jul. 2002.

[11] Nicholas J. Agard, and Jennifer A. Prescher, and C. R. Bertozzi*, "A Strain-Promoted [3 + 2] Azide−Alkyne Cycloaddition for Covalent Modification of Biomolecules in Living Systems," 2004.

[12] H. Meier, H. Petersen, and H. Kolshorn, "Die Ringspannung von Cycloalkinen und ihre spektroskopischen Auswirkungen," *Chem. Ber.*, vol. 113, no. 7, pp. 2398–2409, Jul. 1980.

[13] N. K. Devaraj, R. Weissleder, and S. A. Hilderbrand, "Tetrazine-Based Cycloadditions: Application to Pretargeted Live Cell Imaging," *Bioconjug. Chem.*, vol. 19, no. 12, pp. 2297–2299, Dec. 2008.

[14] M. L. Blackman, M. Royzen, and J. M. Fox, "Tetrazine Ligation: Fast Bioconjugation Based on Inverse-Electron-Demand Diels−Alder Reactivity," *J. Am. Chem. Soc.*, vol. 130, no. 41, pp. 13518–13519, Oct. 2008.

[15] J. Sauer, D. K. Heldmann, J. Hetzenegger, J. Krauthan, H. Sichert, and J. Schuster, "1,2,4,5-Tetrazine: Synthesis and Reactivity in [4+2] Cycloadditions," *European J. Org. Chem.*, vol. 1998, no. 12, pp. 2885–2896, Dec. 1998.

[16] G. Graziano, "Rate enhancement of Diels–Alder reactions in aqueous solutions," *J. Phys. Org. Chem.*, vol. 17, no. 2, pp. 100–101, Feb. 2004.

[17] D. C. Rideout and R. Breslow, "Hydrophobic acceleration of Diels-Alder reactions," *J. Am. Chem. Soc.*, vol. 102, no. 26, pp. 7816–7817, Dec. 1980.

[18] O. Diels and K. Alder, "Synthesen in der hydroaromatischen Reihe," *Justus Liebig's Ann. der Chemie*, vol. 460, no. 1, pp. 98–122, Jan. 1928.

[19] Z. M. Png, H. Zeng, Q. Ye, and J. Xu, "Inverse-Electron-Demand Diels–Alder Reactions: Principles and Applications," *Chem. - An Asian J.*, vol. 12, no. 17, pp. 2142–2159, 2017.

[20] W. E. Bachmann and N. C. Deno, "The Diels--Alder Reaction of 1-Vinylnaphthalene with

α,β- and α,β,γ,δ-Unsaturated Acids and Derivates," *J. Am. Chem. Soc.*, vol. 71, no. 9, pp. 3062–3072, Sep. 1949.
[21] X. Jiang and R. Wang, "Recent developments in catalytic asymmetric inverse-electron-demand diels-alder reaction," *Chem. Rev.*, vol. 113, no. 7, pp. 5515–5546, 2013.
[22] M. R. Karver, R. Weissleder, and S. A. Hilderbrand, "Synthesis and Evaluation of a Series of 1,2,4,5-Tetrazines for Bioorthogonal Conjugation," *Bioconjug. Chem.*, vol. 22, no. 11, pp. 2263–2270, Nov. 2011.
[23] B. L. Oliveira, Z. Guo, and G. J. L. Bernardes, "Inverse electron demand Diels–Alder reactions in chemical biology," *Chem. Soc. Rev.*, vol. 46, no. 16, pp. 4895–4950, Aug. 2017.
[24] F. Thalhammer, U. Wallfahrer, and J. Sauer, "Reaktivität einfacher offenkettiger und cyclischer dienophile bei Diels-Alder-reaktionen mit inversem elektronenbedarf," *Tetrahedron Lett.*, vol. 31, no. 47, pp. 6851–6854, Jan. 1990.
[25] M. T. Taylor, M. L. Blackman, O. Dmitrenko, and J. M. Fox, "Design and Synthesis of Highly Reactive Dienophiles for the Tetrazine– *trans*- Cyclooctene Ligation," *J. Am. Chem. Soc.*, vol. 133, no. 25, pp. 9646–9649, Jun. 2011.
[26] A. Darko *et al.*, "Conformationally Strained trans-Cyclooctene with Improved Stability and Excellent Reactivity in Tetrazine Ligation.," *Chem. Sci.*, vol. 5, no. 10, pp. 3770–3776, Oct. 2014.
[27] M. B. Smith and J. March, *March's Advanced Organic Chemistry: Reactions, Mechanisms, and Structure: Sixth Edition*, vol. 9780471720. 2006.
[28] R. M. Versteegen, R. Rossin, W. ten Hoeve, H. M. Janssen, and M. S. Robillard, "Click-to-release: Instantaneous Doxorubicin Elimination upon Tetrazine Ligation," *Angew. Chemie Int. Ed.*, vol. 52, no. 52, pp. 14112–14116, Dec. 2013.
[29] R. Rossin *et al.*, "Triggered Drug Release from an Antibody–Drug Conjugate Using Fast 'Click-to-Release' Chemistry in Mice," *Bioconjug. Chem.*, vol. 27, no. 7, pp. 1697–1706, Jul. 2016.
[30] J. A. Joule, K. Mills, J. A. Joule, and K. Mills, *Adv. Heterocyclic Chemistry.* Wiley, 2013.
[31] A. K. Steiger, Y. Yang, M. Royzen, and M. D. Pluth, "Bio-orthogonal 'click-and-release' donation of caged carbonyl sulfide (COS) and hydrogen sulfide (H_2S)," *Chem. Commun.*, vol. 53, no. 8, pp. 1378–1380, Jan. 2017.
[32] X. Fan *et al.*, "Optimized Tetrazine Derivates for Rapid Bioorthogonal Decaging in Living Cells," *Angew. Chemie Int. Ed.*, vol. 55, no. 45, pp. 14046–14050, Nov. 2016.
[33] J. C. T. Carlson, H. Mikula, and R. Weissleder, "Unraveling Tetrazine-Triggered Bioorthogonal Elimination Enables Chemical Tools for Ultrafast Release and Universal Cleavage," *J. Am. Chem. Soc.*, p. jacs.7b11217, Feb. 2018.
[34] R. C. Hayward and G. H. Whitham, "trans-Cycloalkenes. Part VI. Addition of iodine(I) azide to trans-cyclo-octene," *J. Chem. Soc. Perkin Trans. 1*, vol. 0, no. 22, p. 2267, Jan. 1975.
[35] Maksim Royzen, and Glenn P. A. Yap, and J. M. Fox*, "A Photochemical Synthesis of Functionalized trans-Cyclooctenes Driven by Metal Complexation," 2008.
[36] Y. Inoue, S. Takamuku, Y. Kunitomi, and H. Sakurai, "Singlet photosensitization of simple alkenes. Part 1. cis–trans-Photoisomerization of cyclo-octene sensitized by aromatic esters," *J. Chem. Soc., Perkin Trans. 2*, no. 11, pp. 1672–1677, 1980.
[37] S. Goto, S. Takamuku, H. Sakurai, Y. Inoue, and T. Hakushi, "Singlet photosensitization of simple alkenes. Part 2. Photochemical transformation of cyclo-octa-1,5-dienes sensitized by aromatic ester," *J. Chem. Soc. Perkin Trans. 2*, no. 11, p. 1678, 1980.
[38] D. Svatunek *et al.*, "Efficient low-cost preparation of trans-Cyclooctenes using a

simplified flow setup for photoisomerization," *Monatshefte für Chemie - Chem. Mon.*, vol. 147, no. 3, pp. 579–585, Mar. 2016.
[39] E. Saxon and C. R. Bertozzi, "Cell Surface Engineering by a Modified Staudinger Reaction."
[40] A. A. Neves *et al.*, "Imaging sialylated tumor cell glycans in vivo."
[41] N. K. Devaraj, R. Upadhyay, J. B. Haun, S. A. Hilderbrand, and R. Weissleder, "Fast and Sensitive Pretargeted Labeling of Cancer Cells through a Tetrazine/ *trans* -Cyclooctene Cycloaddition," *Angew. Chemie Int. Ed.*, vol. 48, no. 38, pp. 7013–7016, Sep. 2009.
[42] R. Rossin *et al.*, "In Vivo Chemistry for Pretargeted Tumor Imaging in Live Mice," *Angew. Chemie Int. Ed.*, vol. 49, no. 19, pp. 3375–3378, Apr. 2010.
[43] R. Rossin and M. S. Robillard, "Pretargeted imaging using bioorthogonal chemistry in mice," *Curr. Opin. Chem. Biol.*, vol. 21, pp. 161–169, 2014.
[44] E. E. Kim, D.-S. Lee, U. Tateishi, and R. P. Baum, *Handbook of nuclear medicine and molecular imaging : principles and clinical applications*. .
[45] J. V. Hiltunen, "Search for New and Improved Radiolabeling Methods for Monoclonal Antibodies: A Review of Different Methods," *Acta Oncol. (Madr).*, vol. 32, no. 7–8, pp. 831–839, Jan. 1993.
[46] A. R. Fritzberg, R. W. Berninger, S. W. Hadley, and D. W. Wester, "Approaches to Radiolabeling of Antibodies for Diagnosis and Therapy of Cancer," *Pharm. Res.*, vol. 5, no. 6, pp. 325–334, 1988.
[47] R. Weissleder, "A clearer vision for in vivo imaging," *Nat. Biotechnol.*, vol. 19, no. 4, pp. 316–317, Apr. 2001.
[48] R. Weissleder and V. Ntziachristos, "Shedding light onto live molecular targets," *Nat. Med.*, vol. 9, no. 1, pp. 123–128, Jan. 2003.
[49] J. A. Woyach *et al.*, "Bruton's tyrosine kinase (BTK) function is important to the development and expansion of chronic lymphocytic leukemia (CLL)," *Blood*, vol. 123, no. 8, pp. 1207–1213, Feb. 2014.
[50] R. L. Siegel, K. D. Miller, and A. Jemal, "Cancer statistics, 2015," *CA. Cancer J. Clin.*, vol. 65, no. 1, pp. 5–29, Jan. 2015.
[51] S. A. Rushworth, M. Y. Murray, L. Zaitseva, K. M. Bowles, and D. J. MacEwan, "Identification of Bruton's tyrosine kinase as a therapeutic target in acute myeloid leukemia," *Blood*, vol. 123, no. 8, pp. 1229–1238, Feb. 2014.
[52] A. M. Bogusz *et al.*, "Quantitative Immunofluorescence Reveals the Signature of Active B-cell Receptor Signaling in Diffuse Large B-cell Lymphoma," *Clin. Cancer Res.*, vol. 18, no. 22, pp. 6122–6135, Nov. 2012.
[53] Y.-T. Tai and K. C. Anderson, "Bruton`s tyrosine kinase: oncotarget in myeloma," *Oncotarget*, vol. 3, no. 9, pp. 913–4, Sep. 2012.
[54] M. de Weers *et al.*, "B-cell antigen receptor stimulation activates the human Bruton's tyrosine kinase, which is deficient in X-linked agammaglobulinemia.," *J. Biol. Chem.*, vol. 269, no. 39, pp. 23857–60, Sep. 1994.
[55] M. Spaargaren *et al.*, "The B Cell Antigen Receptor Controls Integrin Activity through Btk and PLCγ2," *J. Exp. Med.*, vol. 198, no. 10, pp. 1539–1550, Nov. 2003.
[56] L. A. Honigberg *et al.*, "The Bruton tyrosine kinase inhibitor PCI-32765 blocks B-cell activation and is efficacious in models of autoimmune disease and B-cell malignancy," *Proc. Natl. Acad. Sci.*, vol. 107, no. 29, pp. 13075–13080, Jul. 2010.
[57] Y. Lou, T. D. Owens, A. Kuglstatter, R. K. Kondru, and D. M. Goldstein, "Bruton's Tyrosine Kinase Inhibitors: Approaches to Potent and Selective Inhibition, Preclinical and Clinical Evaluation for Inflammatory Diseases and B Cell Malignancies."

[58] A. Turetsky, E. Kim, R. H. Kohler, M. A. Miller, and R. Weissleder, “Single cell imaging of Bruton’s Tyrosine Kinase using an irreversible inhibitor,” *Sci. Rep.*, vol. 4, pp. 1–7, 2014.
[59] E. Kim, K. S. Yang, R. H. Kohler, J. M. Dubach, H. Mikula, and R. Weissleder, “Optimized Near-IR Fluorescent Agents for in Vivo Imaging of Btk Expression,” *Bioconjug. Chem.*, vol. 26, no. 8, pp. 1513–1518, Aug. 2015.
[60] P. Y. Bruice, “Organische Chemie.”
[61] S. Dey and P. Garner, “Synthesis of tert-Butoxycarbonyl (Boc)-Protected Purines,” *Quart. Rev. Biophys. Angew. Chem., Int. Ed. Nucleic Acids Res. Bioorg. Med. Chem. Lett. Helv. Chim. Acta Biol. Chem. Tetrahedron Lett. Tetrahedron Lett. J. J. Synlett J.; Maeda Protein Pept. Lett*, vol. 21, no. 5, pp. 369–4015, 1997.
[62] A. J. Bloodworth, T. Melvin, and J. C. Mitchell, “Mechanistic Aspects of Oxygen Transfer by gem -Dialkylperoxonium Ions,” *J. Org. Chem*, vol. 53, pp. 1078–1082, 1988.
[63] C. A. Lipinski, F. Lombardo, B. W. Dominy, and P. J. Feeney, “Experimental and computational approaches to estimate solubility and permeability in drug discovery and development settings,” *Adv. Drug Deliv. Rev.*, vol. 46, no. 1–3, pp. 3–26, Mar. 2001.
[64] G. Lukinavičius *et al.*, “A near-infrared fluorophore for live-cell super-resolution microscopy of cellular proteins,” *Nat. Chem.*, vol. 5, no. 2, pp. 132–139, Feb. 2013.